SERAWG-02-14

2nd Meeting of the Stock and Ecological Risk Assessment Working Group (SERAWG2)

Age-Structured Production Model (ASPM) assessments of the Alfonsino (*Beryx splendens*) resource in the SIOFA area of the Southern Indian Ocean

Relates to agenda item: 3 Working paper

Anabela Brandão, Doug S. Butterworth and Susan Johnston

Abstract

An Age-Structured Production Model is applied to assess the Alfonsino (*Beryx splendens*) resource in the West and East SIOFA areas of the Southern Indian Ocean. Data limitations restrict these applications to deterministic variants, which assume no variation in annual recruitment about the predictions from a stock-recruitment relationship. The models are fitted to the CPUE series and single year of commercial catch length distribution information available. Both West and East stocks are estimated to be at about 60% of their pre-exploitation spawning stock biomass levels, and well above the levels corresponding to MSY (*MSYL*). These results are insensitive to all sensitivities explored, except for changes in the value assumed for natural mortality (*M*). For the Base case assumption of *M*=0.2, projections under constant annual catches up to 40% above the 2018 levels remain above *MSYL* for the next two decades. However, if a less productive situation is assumed (*M*=0.15), there are some cases of spawning biomass dropping below *MSYL* within 10 years for both areas, including even for continuation of the 2018 catch for the East area.

Age-Structured Production Model (ASPM) assessments of the Alfonsino (*Beryx splendens*) resource in the SIOFA area of the Southern Indian Ocean

Anabela Brandão, Doug S. Butterworth and Susan Johnston

Marine Resource Assessment and Management Group (MARAM)
Department of Mathematics and Applied Mathematics
University of Cape Town, Rondebosch, 7701, South Africa
19 March 2020

ABSTRACT

An Age-Structured Production Model is applied to assess the Alfonsino (*Beryx splendens*) resource in the West and East SIOFA areas of the Southern Indian Ocean. Data limitations restrict these applications to deterministic variants, which assume no variation in annual recruitment about the predictions from a stock-recruitment relationship. The models are fitted to the CPUE series and single year of commercial catch length distribution information available. Both West and East stocks are estimated to be at about 60% of their pre-exploitation spawning stock biomass levels, and well above the levels corresponding to MSY (*MSYL*). These results are insensitive to all sensitivities explored, except for changes in the value assumed for natural mortality (*M*). For the Base case assumption of *M*=0.2, projections under constant annual catches up to 40% above the 2018 levels remain above *MSYL* for the next two decades. However, if a less productive situation is assumed (*M*=0.15), there are some cases of spawning biomass dropping below *MSYL* within 10 years for both areas, including even for continuation of the 2018 catch for the East area.

INTRODUCTION

This paper presents quantitative assessments of the Alfonsino resource in the SIOFA area of the Southern Indian Ocean, as provided through the application of an Age-Structured Production Model (ASPM). This approach was chosen because Alfonsino is a fairly long-lived species, and the approach allows for the effects of delays to be taken into account, as well as the pattern of selectivity by age of the fleets. The model is however deterministic, i.e. no annual variation about the stock recruitment relationship is allowed, as there are no data available upon which the estimation of such variation might be based.

The assessments of the Alfonsino resource presented in this paper have been carried out on a calendar year basis. The ASPM approach takes historical catches into account. In the absence of any information on abundance in terms of trend (or in absolute terms such as tonnes), this (or indeed any other approach with further information or assumptions) cannot provide information on stock productivity or status (e.g. estimates of MSY or of abundance relative to the level yielding MSY, B_{MSY}). To improve this situation, despite misgivings about CPUE as an index of abundance for Alfonsino, these data are also used for the assessments that follow, and especially for the Base case for each of the West and the East areas. Sensitivity tests of these Base cases are also carried out to investigate various aspects of the assessments, including the extent to which varying the estimates of status provided by these Base cases remains consistent with the CPUE information.

Spawning biomass depletion projections under constant catches at the 2018 level of catches (catch for 2018) as well as for several variants thereof are provided for both the West and the East areas. These projections are shown for the Base case as well as the two most influential sensitivities - those for which natural mortality is assumed to be 0.15 or 0.25 instead of 0.2. Retrospective analyses are also conducted for the Base case for the West and East areas.

The nomenclature used in this paper considers the "fishery" in either the West or the East area to be comprised of different "fleets", each of which correspond to a specific country (or to other member or non-member countries). There are CPUE series corresponding to those specific countries, with any of the country, fleet or CPUE series referred to by S1, S2 or S3.

DATA

Catches

Catches start from 1977. Table 1 shows the catch (removals) figures for each of the three fleets for which CPUE data are available, as well as catches from other member and non-member countries. In this Table, the catches in the West from other member countries which are not included in S1, S2 or S3 have been added to those of non-member countries to readily fit all the information in one table. Pre-2001 these catches are all from non-member countries, and post-2001 are all from other member countries. In 2001 a very small amount of the catch comes from other member countries. In the East there are no other member catches.

CPUE

Relative abundance indices obtained from the CPUE standardisation procedure presented in Brandão and Butterworth (2020) for the preferred models are used in fitting the ASPM. The preferred standardisation models are a Negative Binomial model for series with few zero catches and the Hurdle-Negative Binomial for series with a large number of zeros (Brandão and Butterworth, 2020). For readers' convenience, these standardised series are reproduced here in Table 2. While, as mentioned above, there are concerns as to whether these CPUE indices are proportional to fish abundance, the values in Table 2 make this assumption for the analyses that follow, given the absence of any other data related to abundance trends. In the assessment of the East area, the CPUE series for S2 is not used as those data are very sparse and could hardly provide as reliable trend information.

Catch-at-length data

Catch-at-length information is available for the S1 fleet for 2018 only, and the ASPM is fitted to this to estimate fishing selectivity curve. As catch-at-length data are not available for the other two fleets (or other members or non-members), the same selectivity curve is assumed to apply for those fleets as well. A relative weight (w_{len}) of 1.0 for the catch-at-length contribution to the log-likelihood has been applied in this paper, effectively assuming these data to be uncorrelated.

ASSESSMENT METHODOLOGY

The generalised ASPM methodology incorporates all of the abundance indices available for the area (West or East) assessed, so that their information can be incorporated in these ASPM assessments. Appendix 1 describes the ASPM methodology for a multiple fleet fishery. The biological parameter values assumed are based upon values reported for the Alfonsino resource in the SIOFA area (Table 3). Note that the length-weight relationship given by Ivanin and Rebyk (2012) has been converted from kg to tonnes and from standard length to fork length.

Several sensitivity tests have been conducted to better understand various aspects of the assessment. These sensitivity tests are as follows.

For the West

i) Omit the S1 CPUE as it has a different trend to the other series.
ii) For S3, fit to the standardised CPUE series that takes bycatch into account, as this standardised series does not have an unusually high estimated index value in 2011.
iii) Omit the S1 2011 CPUE index to take out the high peak estimated in 2011.

iv) Omit the non-member catches as there is uncertainty about their accuracy.
v) Assume a natural mortality (*M*) of 0.15.
vi) Assume a natural mortality (*M*) of 0.25.
vii) Assume a steepness (*h*) of 0.65.
viii) Assume a steepness (*h*) of 0.85.
ix) Force the spawning biomass depletion in 2018 to be 0.5.
x) Force the spawning biomass depletion in 2018 to be 0.55.
xi) Force the spawning biomass depletion in 2018 to be 0.65.
xii) Force the spawning biomass depletion in 2018 to be 0.7.

For the East

i) Omit the S3 2003 CPUE index to exclude the high peak estimated for that year.
ii) Assume a natural mortality (*M*) of 0.15.
iii) Assume a natural mortality (*M*) of 0.25.
iv) Assume a steepness (*h*) of 0.65.
v) Assume a steepness (*h*) of 0.85.
vi) Force the spawning biomass depletion in 2018 to be 0.5.
vii) Force the spawning biomass depletion in 2018 to be 0.55.
viii) Force the spawning biomass depletion in 2018 to be 0.65.
ix) Force the spawning biomass depletion in 2018 to be 0.7.

In the results that follow, annual fishing intensity has not been expressed as the conventional fishing mortality rate, but rather as an average fishing proportion *F**, which is defined as catch divided by spawning biomass at the start of the year concerned. There are two reasons for this. First, the assessment model treats fishing as a pulse fishery at the start of the year (see Appendix 1), so that *F* there refers to the annual fishing proportion, rather than to the fishing mortality rate. Though that proportion could be transformed to the standard instantaneous rate, that would then refer to the rate at the apical age of the selectivity curve (here the largest age considered); as such it would reflect the fishing intensity on the largest ages which make up only a small proportion of the catch. Hence, reporting the fishing intensity as an average proportion (effectively reflecting a much wider age range) would seem to offer more readily interpretable results.

RESULTS AND DISCUSSION

West area

Table 4 shows the results for the Base case three-fleet assessment of the Alfonsino resource in the West area, as well as four sensitivities, each one assuming some change to the input data for the assessment. All these assessments suggest the current (start of 2019) status of the resource to be very close to 60% of its pre-exploitation equilibrium spawning biomass, a value which has increased very slightly from that at the start of 2018.

Figure 1 shows the estimated spawning biomass (with confidence limits) and recruitment trends for the Base case. Fits to the CPUE data are shown in Figure 2 for the Base case. The model does not fit the CPUE indices for the S1 fleet at all well; this series shows an overall increasing trend and quite variable values especially in the middle period of 2009 to 2013. The model also fails to fit the comparatively very high 2011 CPUE value in the S3 fleet. These poor fits lead to high σ_{CPUE} values for the S1 and S3 series compared to the S2 series, so that more weight is accorded to the last in fitting the model to the data. Fitting to the S3 CPUE indices which are adjusted for bycatch (and does not have the very large peak in 2011) does improve the fit to the S3 CPUE indices (see the σ_{CPUE} values in Table 4).

The fit of the Base case to the catch-at-length distribution for S1 in 2018 is shown in Figure 3. The model fits the catch-at-length data reasonably well. The selectivity function estimated for the Base case is shown in Figure 4.

Figure 5a compares the spawning biomass depletion trajectory for the Base case with those for the four sensitivity tests reported in Table 4. Apart from the sensitivity test which omits the uncertain non-member catches from the assessment, the results are barely distinguishable from those for the Base case. Comparison of the Base case results to those when omitting non-member catches reflects the impact of the (uncertain) catches in the initial period on the assessment; as 2019 is approached, there is little difference between these two trajectories.

Tables 5 and 6 show the results for eight other sensitivity tests performed, which are all variants of the Base case. For ready comparison, results for the Base case are reproduced in these Tables as well. The sensitivity tests reported in Table 5 assume alternative values for natural mortality (*M*) or for the stock-recruitment steepness parameter (*h*). Figure 5b compares the spawning biomass depletion trajectories for the Base case and the four sensitivity tests reported in Tables 5. Results for the two alternative values of steepness are barely distinguishable from the Base case. However, the value assumed for natural mortality has a large impact on the estimated status of the resource. A slight improvement in the fit to the CPUE series is achieved when assuming a higher natural mortality rate, and a slightly worse fit for a lower value of *M* (Table 5).

Table 6 and Figure 5c show results for sensitivity tests that use the addition of a penalty function to the negative log-likelihood to force the spawning biomass depletion in 2018 to specific values. Fixing depletion values in 2018 to values either higher or lower than the value estimated for the Base case results in a deterioration in the fits to the catch-at-length data and the CPUE data, especially for a higher depletion value of 0.7 (Table 6).

Figure 5d shows spawning biomass depletion trajectories for the Base case and for two retrospective analyses: one to 2014 and the other to 2016. As further data become available, the estimated status of the resource over the last two decades improves slightly. Note that so as not to lose the information contained in the 2018 catch-at-length data and so be able to estimate selectivity, for these retrospective analyses those data were assumed to apply to the last year considered.

East area

Table 7 shows the results for the Base case two-fleet assessment of the Alfonsino resource in the East area, as well as four sensitivities. One sensitivity test assumes a change to the S3 CPUE series (omitting the peak value in 2003), while the other sensitivity tests assume alternative values for natural mortality (*M*) or for the stock-recruitment steepness parameter (*h*). The Base case (as well as the first sensitivity test reported in Table 7) suggest that the current (start of 2019) status of the resource to be at 60% of pre-exploitation equilibrium spawning biomass.

Figure 6 shows estimated spawning biomass (with confidence limits) and recruitment trends for the Base case. Fits to the CPUE data are shown in Figure 7 for the Base case. The model fails to fit the comparatively very high 2003 CPUE value for the S3 fleet. Fitting to the S3 CPUE series when omitting this very large peak in 2003 does improve the fit to this series (see the σ_{CPUE} value and the contribution of the CPUE to the negative log-likelihood function in Table 7).

The fit of the Base case to the catch-at-length distribution for S1 in 2018 is shown in Figure 8. The model fits the catch-at-length data reasonably well. The selectivity function estimated for the Base case is shown in Figure 9.

Figure 10a compares the spawning biomass depletion trajectory for the Base case with those of the five sensitivity tests reported in Table 7. As was the case for the West area, the results for the two alternative values of steepness are barely distinguishable from those for the Base case. However, the value assumed for natural mortality has a large impact on the estimated status of the resource. A

slight improvement in the fit to the CPUE series is achieved when assuming a lower natural mortality rate and a slightly better fit for a lower value of *M* (Table 7), the opposite to the direction of this effect in the West area.

Table 8 and Figure 10b show results for sensitivity tests that force the spawning biomass depletion in 2018 to specific values. For ready comparison, results for the Base case are reproduced in this Table and Figure as well. Fixing depletion values in 2018 to values either higher or lower than that estimated for the Base case leads to a deterioration in the fit to the catch-at-length data. Lower assumed values of depletion in 2018 produce worse fits to the CPUE series, but slightly better fits result for higher assumed depletion values (Table 8).

Figure 10c shows spawning biomass depletion trajectories for the Base case and for two retrospective analysis; one up to 2014 and the other up to 2016. The trajectories for the two retrospective analyses are barely distinguishable from each other, and show a slightly higher estimated depletion than for the Base case from about 2005.

Projections

Figure 11a shows spawning biomass depletion trajectories for the Base case for the West area, together with twenty-year projections under constant future annual catches equal to the current (2018) catch as well as for several variants of this value: ±10%, ±20%, ±30% and ±40%. These catches in ascending order are accordingly: 1 294 (i.e. -40%), 1 509, 1 725, 1 940, **2 157** (current), 2 372, 2 587, 2 803 and 3 018 (i.e. +40%) tonnes. Figures 11b and 11c show these projections for the two sensitivities for which natural mortality is assumed to be 0.15 or 0.25 respectively; these particular sensitivities were selected as they make the greatest impact on results. Note that a projection restriction has been applied that does not allow the fully selected fishing proportion to be greater than 90%. Thus, the model builds in a factor to allow for the fact that as abundance declines, it would not be possible to sustain certain levels of removals. This restriction comes into effect for projections for the sensitivity in which *M* = 0.15 and under future catches of +30% and +40% of the current catch level. Figure 11d shows the "model-intended" future catch levels and the actual removals made by the model in these instances. Figure 11e shows average fishing proportion (*F**) trajectories and projections for the Base case. Note that *F** remains below F^*_{MSY} for all these projections.

Similar projections for the East area as for the West area described above are shown in Figures 12a – 12c. The catches considered for the East are in ascending order: 595 (i.e. -40%), 694, 794, 893, **992** (current), 1 091, 1 190, 1 290 and 1 389 (i.e. +40%) tonnes. Note that for the East area the model restriction on the fishing proportion comes into effect for projections for the Base case under future catches of +30% and +40% of the current catch level as well as any future catch level above the current level for the sensitivity in which *M* = 0.15. Figure 12d shows the "model-intended" future catch levels and the actual removals made by the model in the case of the Base case. Figure 12e shows fully selected fishing proportion (*F**) trajectories and projections for the Base case. Note that *F** remains below F^*_{MSY} for most of these projections; however, for the two highest catch levels considered F^*_{MSY} is exceeded after about a decade.

Table 9 lists spawning biomass depletions under these scenarios for the last year for which data are available (2018) and every 5th year thereafter. These are reported for the Base cases for the West and the East areas respectively. For these Base cases the spawning biomass does not drop below *MSYL* for any of the future catch scenarios considered, and the fishing proportion remains below F_{MSY}. However, for the sensitivities corresponding to a less productive resource (*M*=0.15), there are instances where spawning biomass falls below *MSYL* within the next 10 years: for the highest two constant catch options for the West area, and even for the current catch for the East area.

CONCLUSIONS

At their simplest level, these analyses suggest that in both the West and East areas, the Alfonsino resource is at about 60% of its pre-exploitation level, and well above *MSYL* (=B_{MSY}/K). Except in one respect (the value for natural mortality, as discussed below), these results are insensitive to variations in the model and the input data used, and using penalty functions to force current depletion values away from 60% does lead to notable deterioration in the fits to the length distribution and CPUE data input.

The precision of results appears very high (see the CVs reported in, for example, Table 4, which are of the order of some 1% only). This, however, is quite misleading, and reflects a consequence of necessary model simplicity given the limited data, rather than reality. With length distribution data for one year only, there is no basis to estimate the variations about the stock-recruitment relationship that would be present in reality; these, if estimable, would lead to much larger CVs. Furthermore, this model constraint severely restricts the range alternative possible inferences from the length distribution data, which could be impacted by short term variations in recruitment or by selectivity doming. Hence, realistic estimation of the statistical precision of quantities such as current spawning biomass depletion is not possible, and consequently also evaluating the probabilities of, for example, falling below *MSYL* when projecting – deterministic projections are the only meaningful possibility.

However, this does not exclude consideration of the important aspect of sensitivity to model variation, which is certainly consequential in respect of the choice of the value for natural mortality, *M.* Changing *M* from its Base case value of 0.2 to either 0.15 or 0.25 results in changes to the estimated MSY of over 30% for both the West and the East areas. This result should not come as a surprise. The overall situation here is that of the classic stock assessment "one-way-trip". Given essentially only a historical catch series and a downward-trending index of abundance, the estimation of starting biomass and productivity of the resource are confounded – models can satisfactorily estimate values for only two of the three core parameters for starting biomass, productivity and the constant of proportionality for the relative abundance index. This confounding is removed when implementing ASPM by specifying a value for *M*, which is essentially also a measure of a resource's relative productivity – but once that value for *M* is changed, the results for key management-related outcomes change with it.

Risk estimation is necessarily coarse because of the limited data available and the constraints which are therefore placed on the assessment models that can be applied. Consequently, risk evaluation has to be based on deterministic projections. For a range of constant annual catches including up to 40% in excess of those in 2018, spawning biomass remains above *MSYL* for the next two decades for the Base cases for the two areas. However, if less productive resources are assumed (*M* decreased from 0.2 to 0.15), there are some cases of spawning biomass dropping below *MSYL* within 10 years for both areas, including even for continuation of the 2018 catch for the East area.

In relation to future work, and particularly given concerns about often highly variable CPUE indices, the priority should be to obtain some estimates of abundance in absolute terms, possibly by the use of acoustic survey methodology. Given other important uncertainties (such as the most appropriate value to use for natural mortality *M*) further attempted refinement of the existing CPUE data would not be expected to improve the reliability of existing results greatly.

REFERENCES

Brandão, A. and Butterworth, D.S. 2020. Standardised CPUE series of the Alfonsino (*Beryx splendens*) resource in the SIOFA area of the Southern Indian Ocean. Document submitted to SIOFA, March 2020.

Brouwer, S., Wrag, C., Wichman, M, and Nicholas, T. 2020. Alfonsino age and growth – rev1. In prep.

CCSBT (Commission for the Conservation of the Southern Bluefin Tuna). 2003. Report of the Second Meeting of the Management Procedure Workshop. Queenstown, New Zealand, March 2003.

Flores, A, Wiff, R, Galves, P and Diaz, E. 2012. Reproductive biology of alfonsino *Beryx spendens*. J. Fish. Biol. 1:1375-1390.

Ivanin, N and Rebyk, S. 2012. Age, growth parameters and some aspects of reproduction of alfonsino *Beryx splendens* Lowe on the Southwest Indian Ridge. YugNIRO, Ukraine. Working Paper. Workshop on Assessment and Management of Alfonsino Fisheries. FAO, Rome, Italy, 10–12 January 2012. 4 pp.

Lehodey, R., Grandperrin, R. and Marchal, P. 1997. Reproductive biology and ecology of a deep-demersal fish, alfonsina, *Beryx spendens*, over the seamount off New Calendonia. Mar. Biol. 28:17-27.

Table 1. Yearly catches of Alfonsino (in tonnes) estimated to have been taken from the SIOFA area of the Southern Indian Ocean, disaggregated by fleet for years where such information is available, which are used for the analyses conducted in this paper.

Year	West				East			
	S1	S2	S3	Other and non-member	S1	S2	S3	Non-member
1977								522
1978								92
1979								
1980				20.0				
1981				2 524.0				120
1982				921.0				2
1983				852.0				
1984				57.0				
1985				3.0				
1986								
1987				2.0				
1988				16.0				9
1989								
1990								
1991								
1992				314.0				
1993				462.0				
1994				1 534.0				
1995				2 249.0				
1996				3 079.0				
1997				1 031.0				
1998				859.0				
1999			147.9	1 964.0			26.8	
2000			390.2	1 589.0			0.0	
2001		2 986.5	6.4	594.4			1 070.5	
2002		37.3	105.4			248.7	2 871.1	
2003	353.8		3.4		911.5		1 605.9	
2004	141.6		44.7	7.9			824.8	
2005	391.8		32.1	10.1	828.1		182.3	
2006			17.6		164.3		202.6	
2007			96.8	1.2			190.3	
2008			33.1	16.8			173.7	
2009	1 828.5	1 204.2	62.3		368.9		0.0	
2010	2 033.4	977.3	16.2		1 713.9		30.9	
2011	2 672.9	612.3	58.0	147.0	747.2		531.9	
2012	3 101.3	104.5	235.6	561.0	1 244.2	191	46.4	
2013	2 184.0	1 262.8	88.8	718.3	1 127.5	2.1	29.0	
2014	2 405.1	452.1	75.8	1.7	615.4			
2015	2 096.7	2 119.4		0.5	690.7	276.4	59.8	
2016	1 529.6	1 976.9	1.4				12.9	
2017	2 392.7	1 971.8			803.1	80.6		
2018	1 090.4	1 066.3	0.04		692.0	300		
Total	22 221.7	14 771.4	1 415.5	19 535.0	9 906.9	1 098.8	7 858.8	745.0
Grand total	57 943.6				19 609.5			

Table 2. Preferred relative abundance indices for Alfonsino selected from standardisation analyses for commercial CPUE series for the SIOFA area of the Southern Indian Ocean for datasets available for the West and East areas (Brandão and Butterworth, 2020).

Year	West			East	
	S1	**S2**	**S3**	**S1**	**S3**
2001	—	2.088	—	—	—
2002	—	0.819	—	—	0.553
2003	0.143	—	—	1.373	4.450
2004	0.265	—	0.303	—	1.012
2005	0.368	—	0.055	1.503	0.411
2006	—	—	0.132	1.103	0.596
2007	—	—	0.282	—	0.241
2008	—	—	0.060	—	0.404
2009	1.633	2.485	0.438	1.078	—
2010	0.675	0.722	0.276	0.954	0.603
2011	0.942	0.866	6.585	1.096	1.241
2012	1.752	0.478	2.055	1.148	1.098
2013	0.671	1.079	1.305	0.869	1.489
2014	0.846	0.562	0.328	0.716	—
2015	1.191	0.805	—	0.624	0.711
2016	1.480	0.585	0.179	—	0.190
2017	1.800	0.502	—	1.010	—
2018	1.234	1.009	—	0.524	—

Table 3. Biological parameter values assumed for the Base case assessments conducted. Note that for simplicity, maturity is assumed to be knife-edged in age.

Parameter	West	East
Natural mortality M (yr^{-1})[1]	0.2	0.2
von Bertalanffy growth[2]		
ℓ_∞ (cm)	69.21	69.21
κ (yr^{-1})	0.05	0.05
t_0 (yr)	-6.12	-6.12
Weight (in gm) length (in cm) relationship[3]		
c	2.9×10^{-5}	2.9×10^{-5}
d	2.98	2.98
Age at maturity (yr) a_m[4]	6	6
Steepness parameter (h)	0.75	0.75

[1] Taken from TOR document.
[2] Brouwer (2002)
[3] Ivanin and Rebyk (2012)
[4] Lehodey *et al*. (1997); Flores *et al*. (2012)

Table 4. Estimates for a **Base case** three CPUE series (S1, S2 and S3) assessment model (ASPM) for the **West** that assumes the same commercial selectivity for each, when fitted to the CPUE values and the S1 2018 catch-at-length data for Alfonsino from the SIOFA area of the Southern Indian Ocean. Results for some **sensitivities** are also shown. The estimates shown are for the pre-exploitation Alfonsino spawning biomass (K^{sp}), the current spawning stock depletion $\left(B_{2019}^{sp}\right)$ in terms of both K^{sp} and B_{MSY}, and exploitable biomass $\left(B_{2019}^{exp}\right)$ at the beginning of the year 2019 (assuming the same selectivity as for 2018). Estimates of parameters pertinent to fitting the catch-at-length information are also shown, together with contributions to the (negative of the) log-likelihood. Numbers in brackets represent CVs. The details of the various model variants reported are given in the text. Note that $MSYL = B_{MSY}/K$; see text for the definition of F_{MSY}^{*}.

Parameter estimates		Model				
		Base case	**Omit S1 CPUE**	**S3 CPUE adjusted for bycatch**	**Omit S3 2011 CPUE index**	**Omit Non-member catches**
K^{sp} (tonnes)		49 138 (0.031)	48 615 (0.021)	49 089 (0.021)	49 190 (0.022)	47 286 (0.023)
$MSYL^{sp}$		0.292	0.311	0.293	0.292	0.289
B_{1999}^{sp}/K^{sp}		0.873 (0.004)	0.873 (0.004)	0.873 (0.004)	0.874 (0.004)	1.000 (0.000)
B_{2018}^{sp}/K^{sp}		0.598 (0.022)	0.595 (0.017)	0.598 (0.017)	0.598 (0.017)	0.602 (0.018)
B_{2019}^{sp}/K^{sp}		0.607 (0.021)	0.604 (0.017)	0.607 (0.017)	0.607 (0.017)	0.610 (0.017)
B_{2019}^{sp}/B_{MSY}		2.078	1.940	2.072	2.083	2.109
B_{2019}^{exp} (tonnes)		4 578 (0.260)	3 907 (0.187)	4 512 (0.163)	4 650 (0.160)	4 685 (0.147)
σ_{CPUE}	S1	0.981	—	0.983	0.979	1.074
	S2	0.465	0.477	0.466	0.464	0.473
	S3	1.399	1.405	0.848	1.157	1.203
a_{50} (yr)		14.15	14.49	14.18	14.12	14.00
δ (yr^{-1})		1.968	1.962	1.967	1.968	1.969
β		0.051 (0.272)	0.058 (0.008)	0.052 (0.014)	0.050 (0.022)	0.048 (0.021)
σ_{len}		0.045	0.045	0.045	0.046	0.046
-ln *L*: Length		-21.5	-21.9	-21.5	-21.4	-21.1
-ln *L*: CPUE		13.10	7.19	7.15	10.12	11.98
-ln *L*: Total		-8.4	-14.8	-14.4	-11.3	-9.2
MSY (tonnes)		3 325	3 526	3 338	3 313	3 152
F_{MSY}^{*}		0.232	0.233	0.232	0.231	0.231

Table 5. Estimates for further **sensitivity tests** to the **Base case** for the **West**. The details of the various sensitivity tests reported are given in the text.

Parameter estimates		Model				
		Base case	***M* = 0.15**	***M* = 0.25**	**Steepness *h* = 0.65**	**Steepness *h* = 0.85**
K^{sp} (tonnes)		49 138 (0.031)	44 064 (0.017)	58 009 (0.050)	49 531 (0.030)	48 840 (0.031)
$MSYL^{sp}$		0.292	0.325	0.422	0.336	0.321
B^{sp}_{1999}/K^{sp}		0.873 (0.004)	0.834 (0.004)	0.908 (0.005)	0.873 (0.004)	0.874 (0.004)
B^{sp}_{2018}/K^{sp}		0.598 (0.022)	0.450 (0.024)	0.718 (0.020)	0.593 (0.022)	0.602 (0.021)
B^{sp}_{2019}/K^{sp}		0.607 (0.021)	0.451 (0.024)	0.730 (0.019)	0.601 (0.021)	0.612 (0.021)
B^{sp}_{2019}/B_{MSY}		2.078	1.385	1.732	1.790	1.904
B^{exp}_{2019} (tonnes)		4 578 (0.260)	3 351 (0.197)	5 627 (0.331)	4 553 (0.258)	4 597 (0.262)
σ_{CPUE}	S1	0.981	1.067	0.924	0.984	0.979
	S2	0.465	0.525	0.439	0.466	0.465
	S3	1.399	1.405	1.396	1.400	1.398
a_{50} (yr)		14.15	14.37	14.03	14.19	14.12
δ (yr^{-1})		1.968	2.169	1.798	1.978	1.960
β		0.051 (0.272)	0.051 (0.280)	0.054 (0.254)	0.051 (0.273)	0.051 (0.271)
σ_{len}		0.045	0.044	0.046	0.045	0.046
-ln *L*: Length		-21.5	-22.2	-21.2	-21.5	-21.5
-ln *L*: CPUE		13.10	15.70	11.59	13.16	13.05
-ln *L*: Total		-8.4	-6.5	-9.6	-8.3	-8.4
MSY (tonnes)		3 325	2 123	4 931	2 884	3 627
F^{*}_{MSY}		0.232	0.148	0.202	0.173	0.231

Table 6. Estimates for further **sensitivity tests** to the **Base case** for the **West**. The details of the various sensitivity tests reported are given in the text.

Parameter estimates		Model				
		Base case	$B^{sp}_{2018}/K^{sp} = 0.5$	$B^{sp}_{2018}/K^{sp} = 0.55$	B^{sp}_{2018}/K^{sp}=0.65	B^{sp}_{2018}/K^{sp}=0.7
K^{sp} (tonnes)		49 138 (0.031)	40 971 (0.011)	44 517 (0.027)	55 815 (0.030)	67 705 (0.013)
$MSYL^{sp}$		0.292	0.297	0.307	0.290	0.289
B^{sp}_{1999}/K^{sp}		0.873 (0.004)	0.845 (0.002)	0.859 (0.005)	0.889 (0.004)	0.904 (0.000)
B^{sp}_{2018}/K^{sp}		0.598 (0.022)	0.504 (0.010)	0.551 (0.026)	0.650 (0.017)	0.700 (0.000)
B^{sp}_{2019}/K^{sp}		0.607 (0.021)	0.514 (0.010)	0.560 (0.025)	0.659 (0.017)	0.707 (0.000)
B^{sp}_{2019}/B_{MSY}		2.078	1.728	1.823	2.272	2.449
B^{exp}_{2019} (tonnes)		4 578 (0.260)	3 844 (0.260)	3 934 (0.242)	5 876 (0.262)	22 103 (0.179)
σ_{CPUE}	S1	0.981	1.034	1.017	0.936	0.827
	S2	0.465	0.498	0.486	0.447	0.446
	S3	1.399	1.174	1.170	1.141	1.094
a_{50} (yr)		14.15	12.21	13.30	14.91	10.77
δ (yr^{-1})		1.968	1.613	1.793	2.156	1.847
β		0.051 (0.272)	0.101 (0.143)	0.074 (0.169)	0.028 (0.298)	0.026 (0.352)
σ_{len}		0.045	0.070	0.053	0.061	0.093
-ln *L*: Length		-21.5	-8.6	-16.8	-12.6	-0.5
-ln *L*: CPUE		13.1	11.8	11.3	8.9	6.8
Penalty on B^{sp}_{2018}/K^{sp}		—	0.33	4.98	6.50	0.00
-ln *L*: Total		-8.4	3.2[5]	-5.5[5]	-3.7[5]	6.3[5]
MSY (tonnes)		3 325	2 725	2 950	3 778	4 445
F^{*}_{MSY}		0.232	0.224	0.216	0.233	0.227

[5] Note that for better cross-column comparability the contribution to the negative log-likelihood function, the penalty function contribution has been omitted from the calculation of the total negative log-likelihood.

Table 7. Estimates for a **Base case** two CPUE series (S1 and S3) assessment model (ASPM) for the **East** that assumes the same commercial selectivity for each, when fitted to the CPUE values and the S1 2018 catch-at-length data for Alfonsino from the SIOFA area of the Southern Indian Ocean. Results for some **sensitivities** are also shown. The estimates shown are for the pre-exploitation Alfonsino spawning biomass (K^{sp}), the current spawning stock depletion $\left(B_{2019}^{sp}\right)$ in terms of both K^{sp} and B_{MSY}, and exploitable biomass $\left(B_{2019}^{exp}\right)$ at the beginning of the year 2019 (assuming the same selectivity as for 2018). Estimates of parameters pertinent to fitting the catch-at-length information are also shown, together with contributions to the (negative of the) log-likelihood. Numbers in brackets represent CVs. The details of the various model variants reported are given in the text. Note that $MSYL = B_{MSY}/K$.

Parameter estimates		Model					
		Base case	**Omit S3 2003 CPUE index**	***M* = 0.15**	***M* = 0.25**	**Steepness *h* = 0.65**	**Steepness *h* = 0.85**
K^{sp} (tonnes)		15 358 (0.029)	15 428 (0.028)	14 533 (0.013)	17 459 (0.027)	15 421 (0.027)	15 332 (0.017)
$MSYL^{sp}$		0.292	0.293	0.322	0.381	0.334	0.289
B_{1999}^{sp}/K^{sp}		0.998 (0.000)	0.998 (0.000)	0.995 (0.000)	0.999 (0.000)	0.997 (0.000)	0.998 (0.000)
B_{2018}^{sp}/K^{sp}		0.613 (0.020)	0.615 (0.019)	0.458 (0.016)	0.741 (0.011)	0.599 (0.019)	0.625 (0.012)
B_{2019}^{sp}/K^{sp}		0.599 (0.021)	0.601 (0.020)	0.437 (0.018)	0.731 (0.011)	0.583 (0.021)	0.613 (0.012)
B_{2019}^{sp}/B_{MSY}		2.053	2.053	1.354	1.916	1.744	2.120
B_{2019}^{exp} (tonnes)		1 780 (0.251)	1 856 (0.230)	1 447 (0.162)	2 166 (0.161)	1 752 (0.232)	1 825 (0.148)
σ_{CPUE}	S1	0.243	0.242	0.234	0.285	0.239	0.246
	S3	0.779	0.682	0.791	0.787	0.778	0.779
a_{50} (yr)		13.62	13.58	13.56	13.62	13.66	13.67
δ (yr^{-1})		2.048	2.043	2.228	1.883	2.052	2.046
β		0.038 (0.254)	0.036 (0.251)	0.033 (0.207)	0.038 (0.006)	0.037 (0.235)	0.038 (0.011)
σ_{len}		0.028	0.028	0.029	0.027	0.028	0.028
-ln *L*: Length		-37.3	-37.2	-36.3	-37.8	-37.1	-37.5
-ln *L*: CPUE		-7.70	-9.62	-7.98	-5.68	-7.92	-7.55
-ln *L*: Total		-45.0	-46.8	-44.2	-43.5	-45.0	-45.0
MSY (tonnes)		1 010	1 014	696	1 466	894	1 121
F_{MSY}^{*}		0.225	0.225	0.149	0.220	0.174	0.253

Table 8. Estimates for further **sensitivity tests** to the **Base case** for the **East** detailed in the caption to Table 7. The details of the various sensitivity tests reported are given in the text.

Parameter estimates		Model				
		Base case	$B^{sp}_{2018}/K^{sp} = 0.5$	$B^{sp}_{2018}/K^{sp} = 0.55$	B^{sp}_{2018}/K^{sp}=0.65	B^{sp}_{2018}/K^{sp}=0.7
K^{sp} (tonnes)		15 358 (0.029)	12 456 (0.006)	13 452 (0.016)	16832 (0.025)	19 546 (0.007)
$MSYL^{sp}$		0.292	0.302	0.425	0.293	0.291
B^{sp}_{1999}/K^{sp}		0.998 (0.000)	0.997 (0.000)	0.998 (0.000)	0.998 (0.000)	0.998 (0.000)
B^{sp}_{2018}/K^{sp}		0.613 (0.020)	0.500 (0.002)	0.550 (0.018)	0.650 (0.015)	0.700 (0.000)
B^{sp}_{2019}/K^{sp}		0.599 (0.021)	0.481 (0.002)	0.533 (0.019)	0.638 (0.015)	0.690 (0.000)
B^{sp}_{2019}/B_{MSY}		2.053	1.594	1.255	2.177	2.370
$B^{\exp}_{2019}$ (tonnes)		1 780 (0.251)	709 (0.547)	378 (0.503)	2859 (0.142)	5 069 (0.111)
σ_{CPUE}	S1	0.243	0.317	0.347	0.236	0.244
	S3	0.779	0.836	0.898	0.770	0.770
a_{50} (yr)		13.62	13.58	16.34	12.855	11.76
δ (yr^{-1})		2.048	1.860	2.039	1.994	1.923
β		0.038 (0.254)	0.087 (0.144)	0.068 (0.094)	0.027 (0.009)	0.024 (0.197)
σ_{len}		0.028	0.067	0.035	0.034	0.056
-ln *L*: Length		-37.3	-10.7	-30.4	-30.5	-15.4
-ln *L*: CPUE		-7.7	-3.6	-1.6	-8.2	-7.8
penalty on B^{sp}_{2018}/K^{sp}		—	0.03	10.20	7.96	0.00
-ln *L*: Total		-45.0	-14.3[6]	-32.0[6]	-38.7[6]	-23.2[6]
MSY (tonnes)		1 010	826	847	1107	1 285
F^{*}_{MSY}		0.225	0.220	0.148	0.224	0.226

[6] Note that for better cross-column comparability the contribution to the negative log-likelihood function, the penalty function contribution has been omitted from the calculation of the total negative log-likelihood.

Table 9. Spawning biomass depletion for the **Base case** for the current year (2018) and every 5th year thereafter under constant future annual catches of 2 157 tonnes (as for 2018) for the **West area** and 992 tonnes (for 2018) for the **East** area, as well as ±10%, ±20%, ±30% and ±40% of those catches respectively. Note that there are no instances where values drop below *MSYL*.

	Future catch (tonnes)	Current (2018)	2023	2028	2033	2038
West	**1294**	0.598	0.684	0.738	0.771	0.791
	1509	0.598	0.671	0.715	0.743	0.760
	1725	0.598	0.657	0.691	0.713	0.727
	1940	0.598	0.644	0.668	0.683	0.694
	2157	0.598	0.631	0.644	0.653	0.659
	2372	0.598	0.617	0.620	0.622	0.623
	2587	0.598	0.604	0.596	0.590	0.586
	2803	0.598	0.590	0.571	0.558	0.548
	3018	0.598	0.577	0.547	0.525	0.509
East	**595**	0.613	0.634	0.663	0.681	0.693
	694	0.613	0.614	0.627	0.636	0.642
	794	0.613	0.594	0.592	0.589	0.588
	893	0.613	0.575	0.555	0.541	0.531
	992	0.613	0.555	0.519	0.492	0.471
	1091	0.613	0.535	0.482	0.441	0.408
	1190	0.613	0.515	0.444	0.388	0.341
	1290	0.613	0.495	0.406	0.333[7]	0.301[7]
	1389	0.613	0.475	0.367	0.310[7]	0.293[7]

[7] Note that for these years, the model restriction that does not allow the fully selected fishing proportion to be greater than 90% has been enforced.

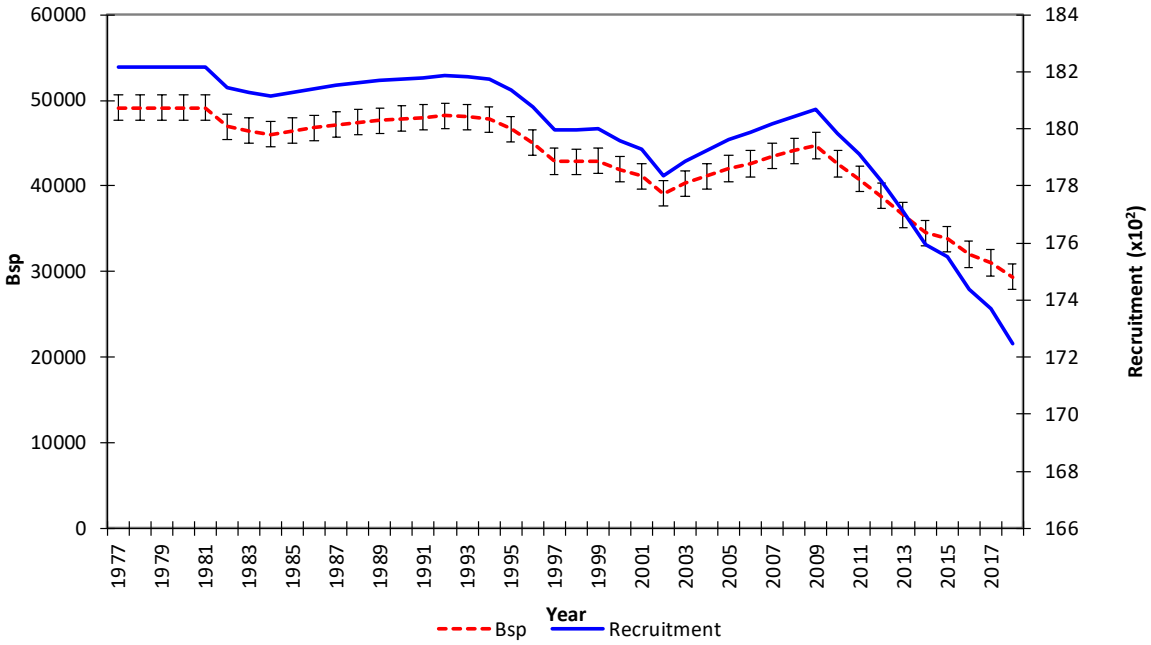

Figure 1. Spawning biomass estimates (dashed line) and estimated recruitment (full line) for the **Base case** three CPUE series model for the **West**. Confidence limits (Hessian-based) of one standard error for the spawning biomass are also shown.

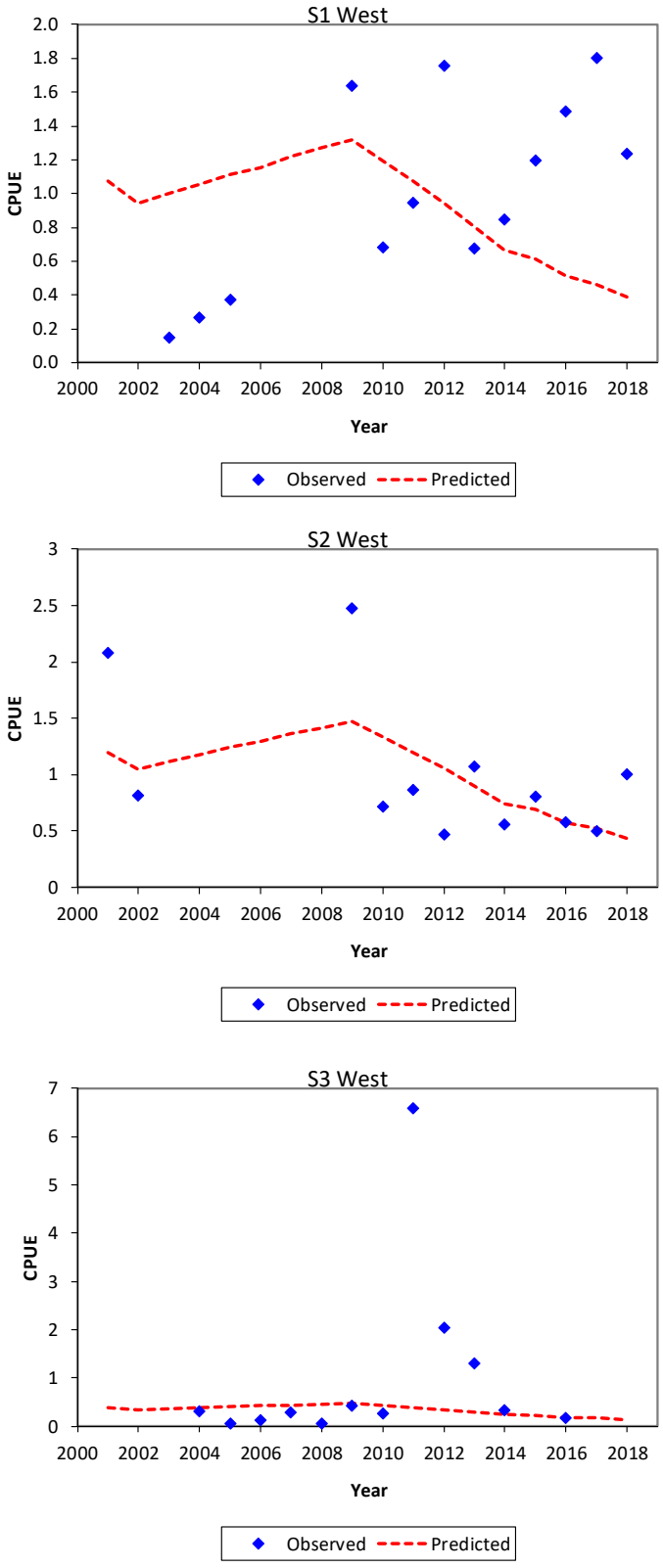

Figure 2. Exploitable biomass and the GLM-standardised CPUE series to which the model is fit (divided by the corresponding estimated catchability *q* values to express them in biomass units) for the **Base case** for the **West**.

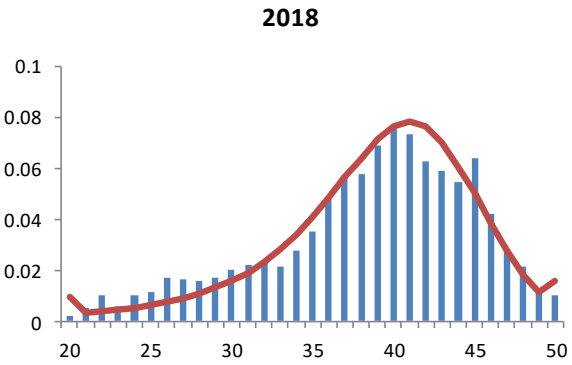

Figure 3. Assessment predictions (curve) for the annual catch-at-length proportions (bars) in 2018 for **S1 West** for the **Base case**. Note that lengths below 20 and above 50 cm have been combined into minus- and plus-groups respectively.

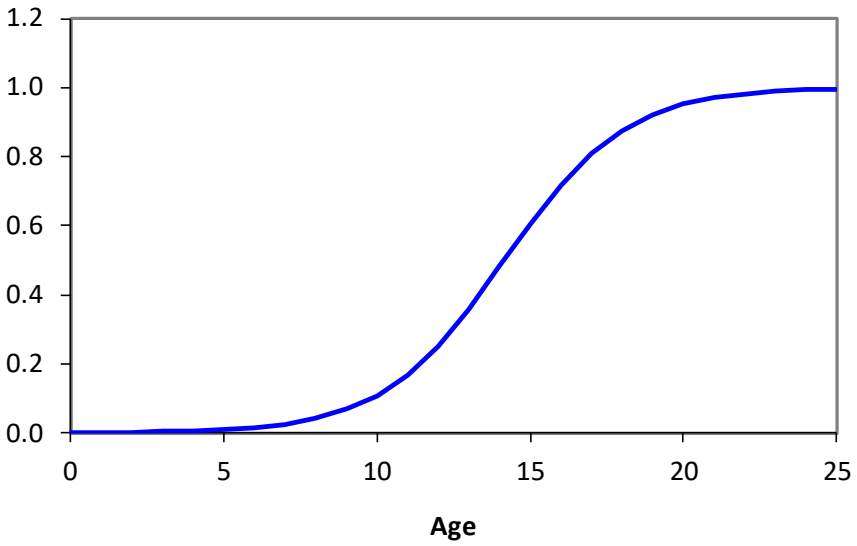

Figure 4. Estimated selectivity curve for S1 **West** for the **Base case**.

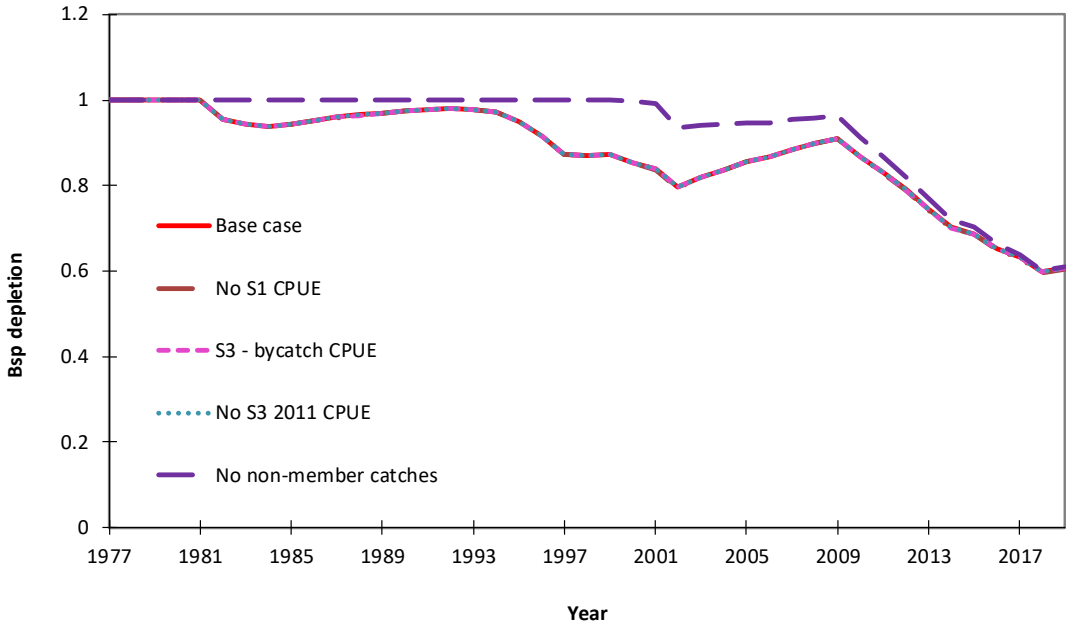

Figure 5a. Spawning biomass depletion estimates for the **Base case** for the **West** as well as for four **sensitivity tests:** 1) omit S1 CPUE, 2) use S3 CPUE adjusted for bycatch, 3) omit S3 2011 CPUE index and 4) omit non-member catches. Note that results for the Base case and the first three sensitivities are barely distinguishable.

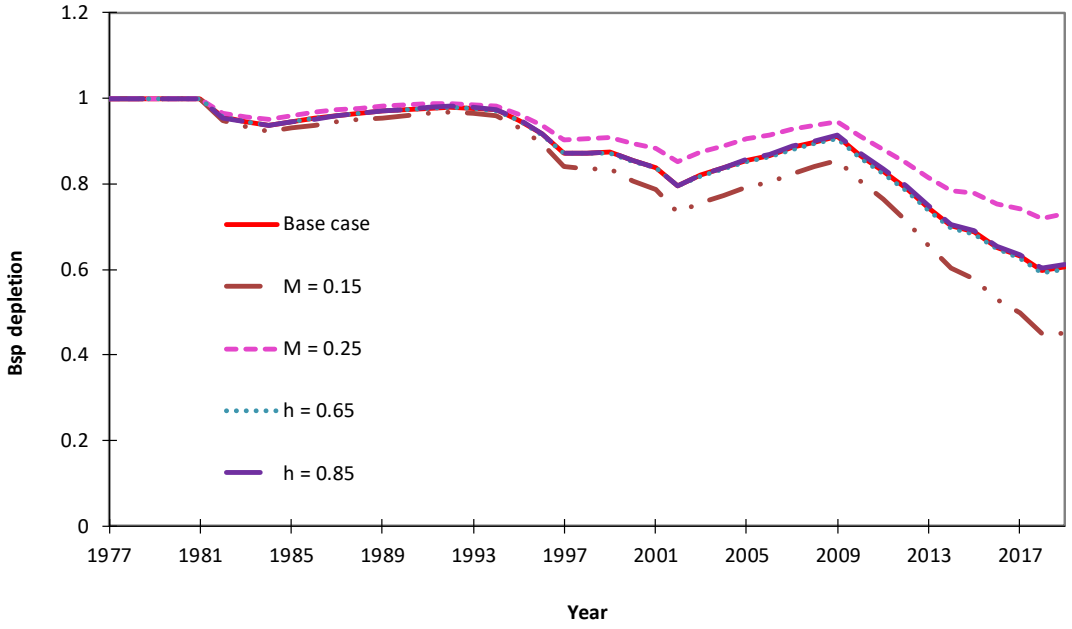

Figure 5b. Spawning biomass depletion estimates for the **Base case** for the **West** as well as for four **sensitivity tests:** 1) M = 0.15, 2) M = 0.15, 3) h = 0.65 and 4) h = 0.85. Note that the results for the two alternative values of steepness are barely distinguishable from those for the Base case.

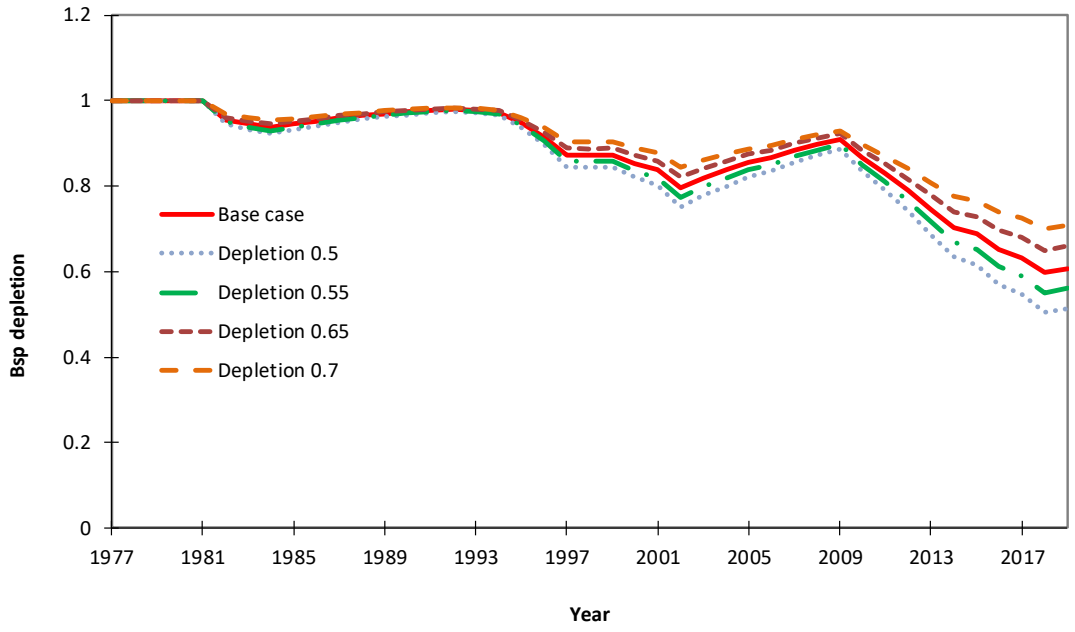

Figure 5c. Spawning biomass depletion estimates for the **Base case** for the **West** as well as for four **sensitivity tests:** 1) $B^{sp}_{2018}/K^{sp} = 0.5$, 2) $B^{sp}_{2018}/K^{sp} = 0.55$, 3) $B^{sp}_{2018}/K^{sp} = 0.65$ and 4) $B^{sp}_{2018}/K^{sp} = 0.7$.

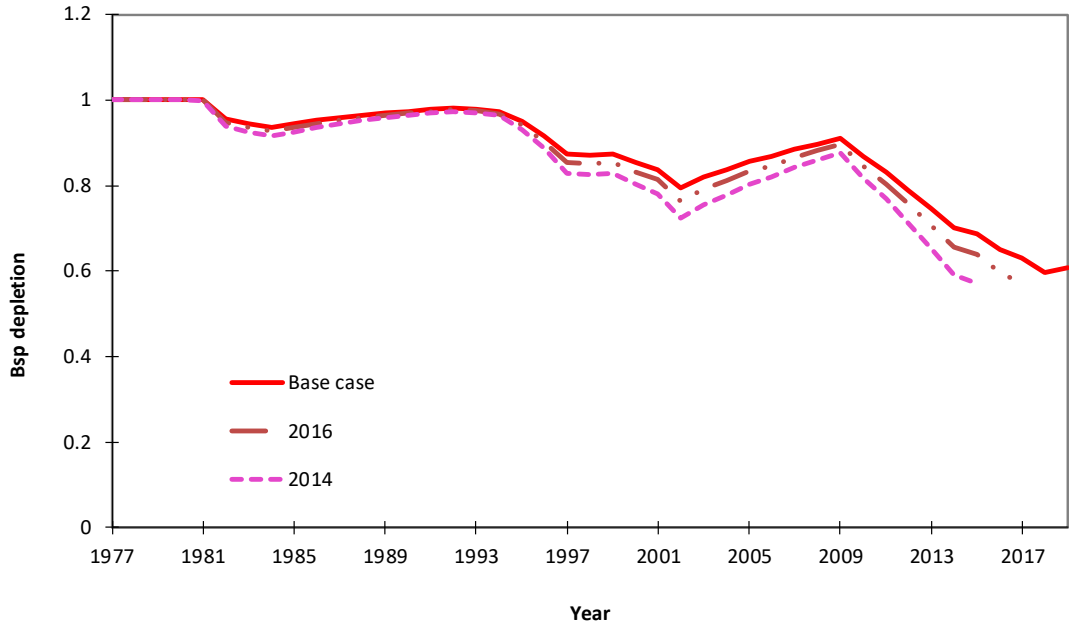

Figure 5d. Comparison of spawning biomass depletion trajectories for the **Base case** for the **West** and for two retrospective analyses.

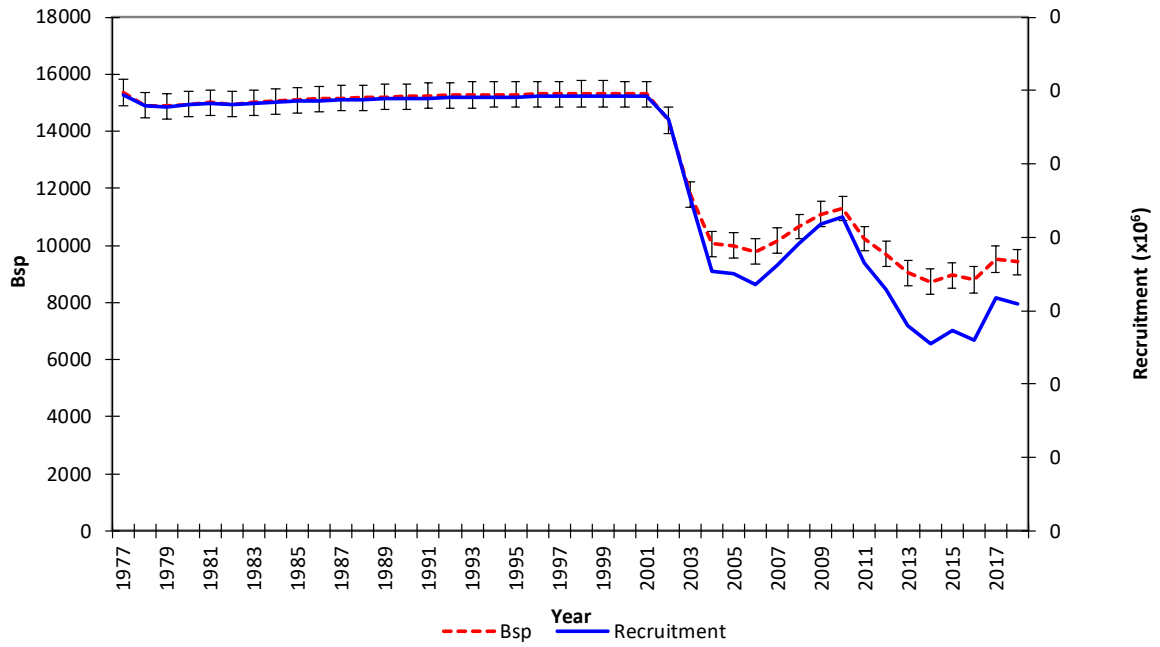

Figure 6. Spawning biomass estimates (dashed line) and estimated recruitment (full line) for the **Base case** for the **East** model for two CPUE series. Confidence limits (Hessian-based) of one standard error for the spawning biomass are also shown.

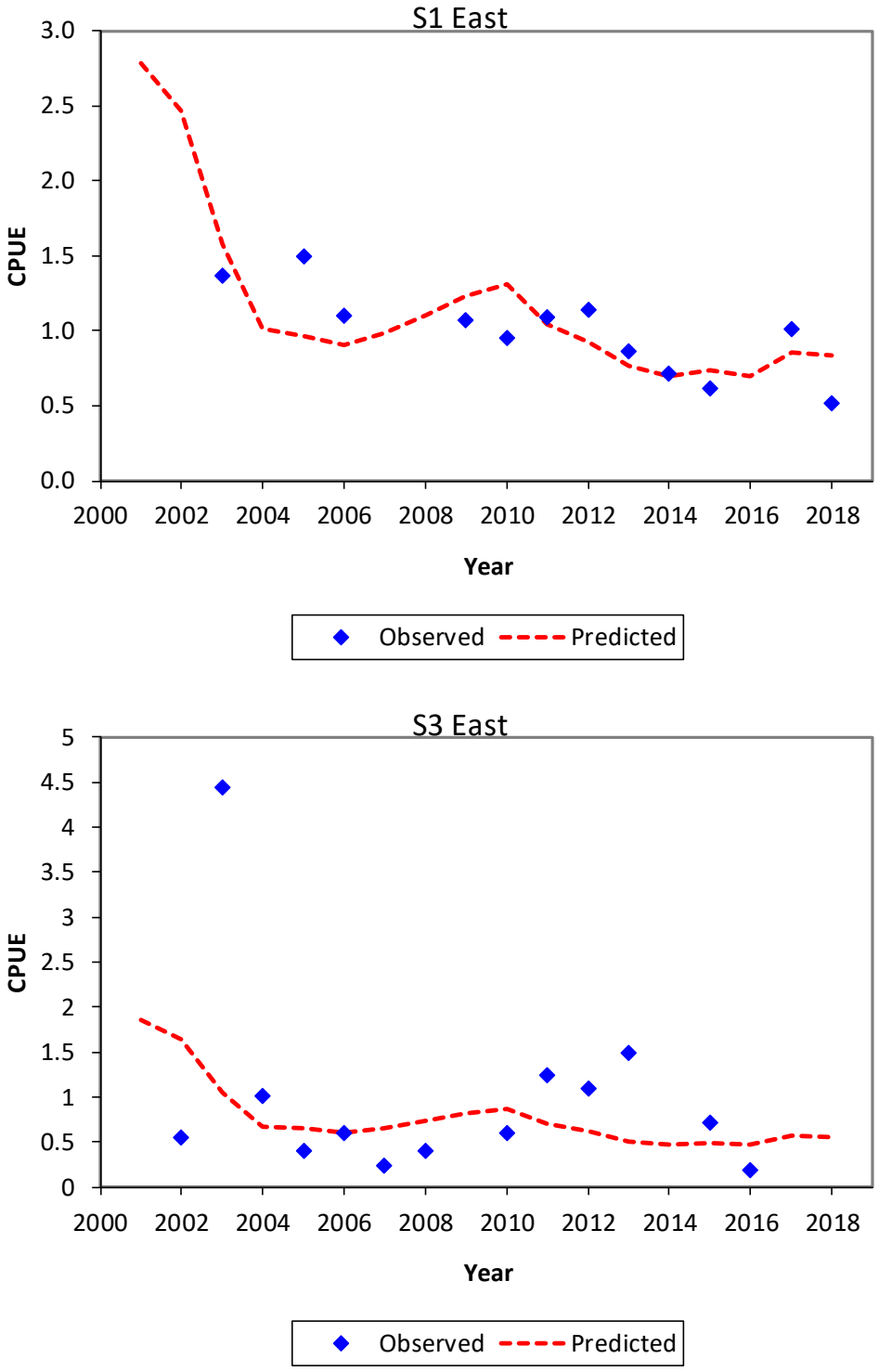

Figure 7. Exploitable biomass and the GLM-standardised CPUE series to which the model is fit (divided by the corresponding estimated catchability *q* values to express them in biomass units) for the **Base case** for the **East**.

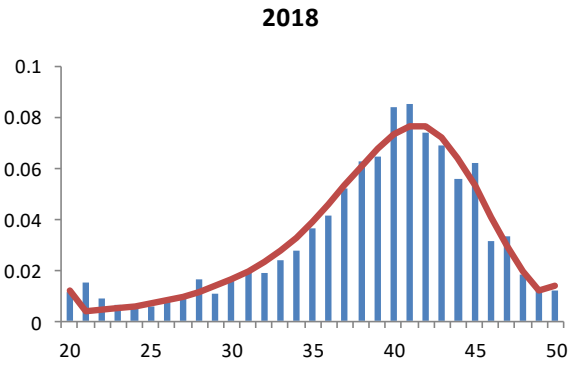

Figure 8. Assessment predictions (curve) for the annual catch-at-length proportions (bars) in 2018 for **S1 East** for the **Base case**. Note that lengths below 20 and above 50 cm have been combined into minus- and plus-groups respectively.

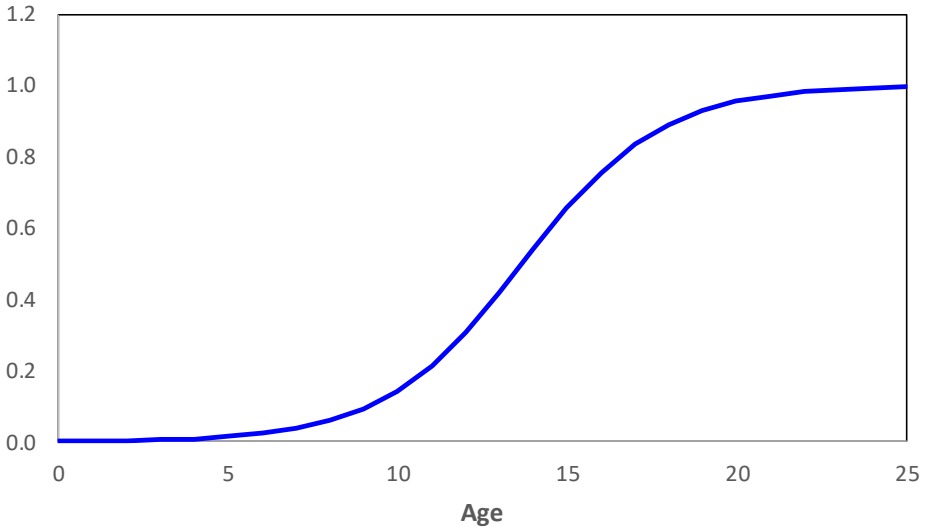

Figure 9. Estimated selectivity curve for S1 **East** for the **Base case**.

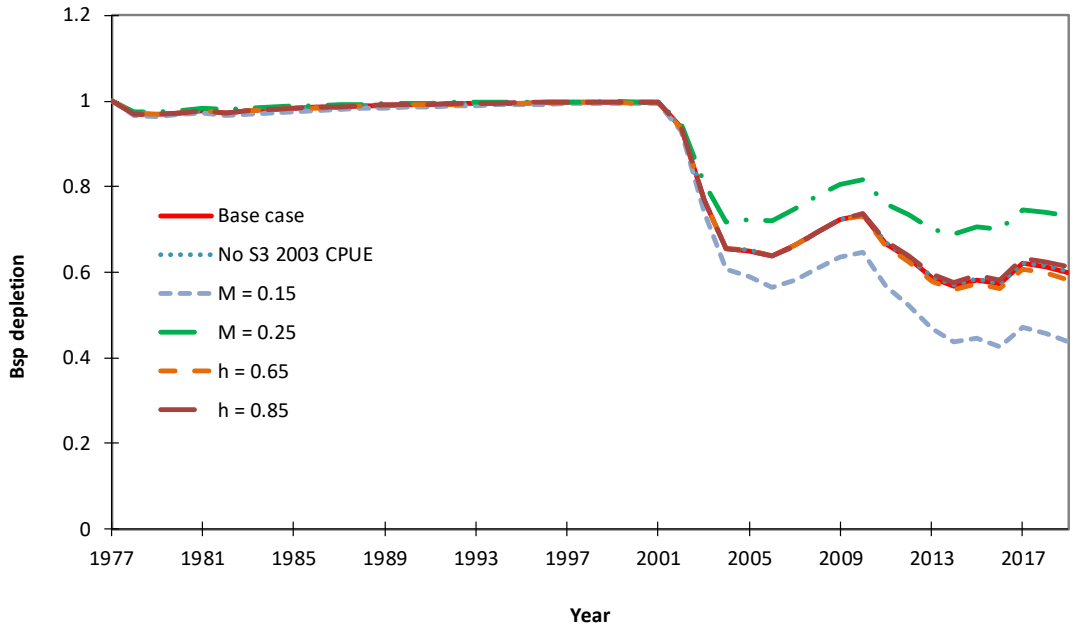

Figure 10a. Spawning biomass depletion estimates for the **Base case** for the **East** as well as for five **sensitivity tests:** 1) omit S3 2003 CPUE index, 2) *M* = 0.15, 3) *M* = 0.25, 4) *h* = 0.65 and 5) *h* = 0.85. Note that all results except those from the different *M* values are barely distinguishable from those for the Base case.

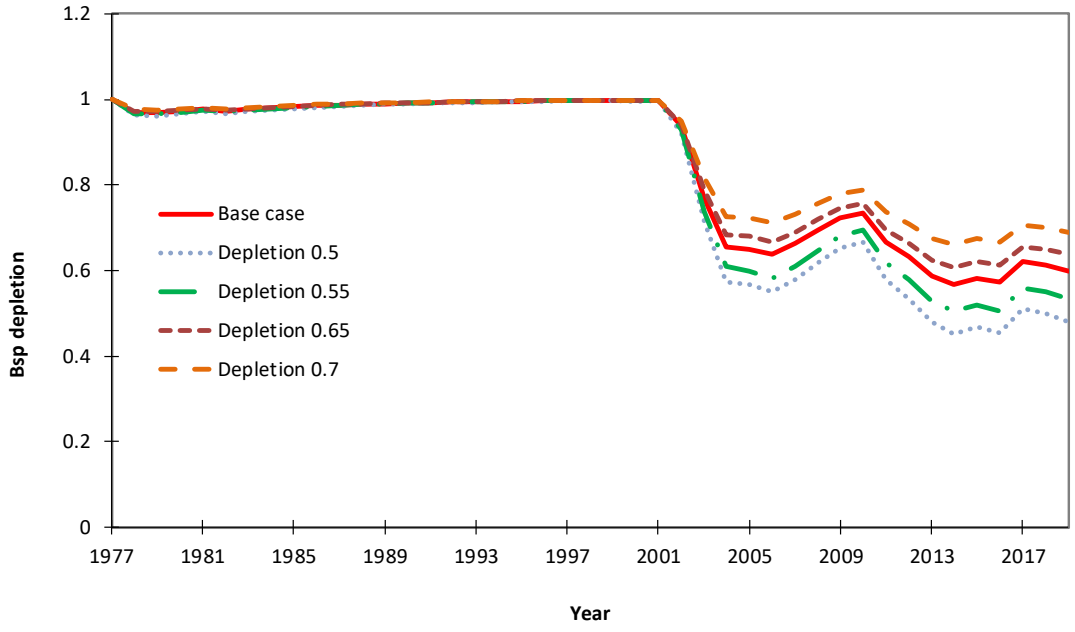

Figure 10b. Spawning biomass depletion estimates for the **Base case** for the **East** as well as four **sensitivity tests:** 1) $B^{sp}_{2018}/K^{sp} = 0.5$, 2) $B^{sp}_{2018}/K^{sp} = 0.55$, 3) $B^{sp}_{2018}/K^{sp} = 0.65$ and 4) $B^{sp}_{2018}/K^{sp} = 0.7$.

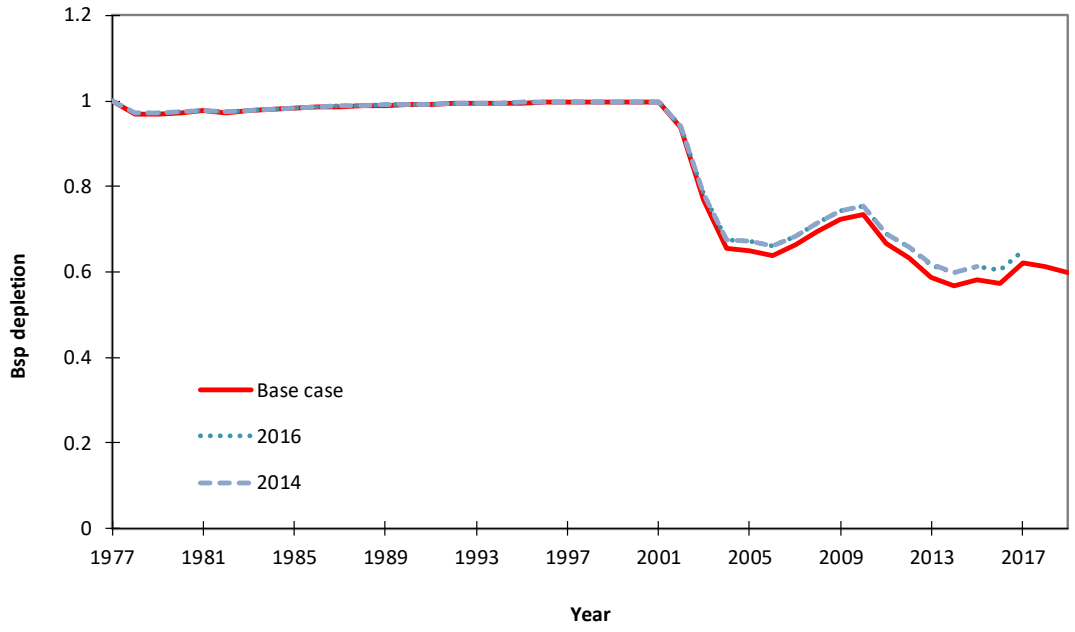

Figure 10c. Comparison of spawning biomass depletion trajectories for the **Base case** for the **East** and for two **retrospective analyses**. Note that the trajectories for the two retrospective analyses are barely distinguishable from each other.

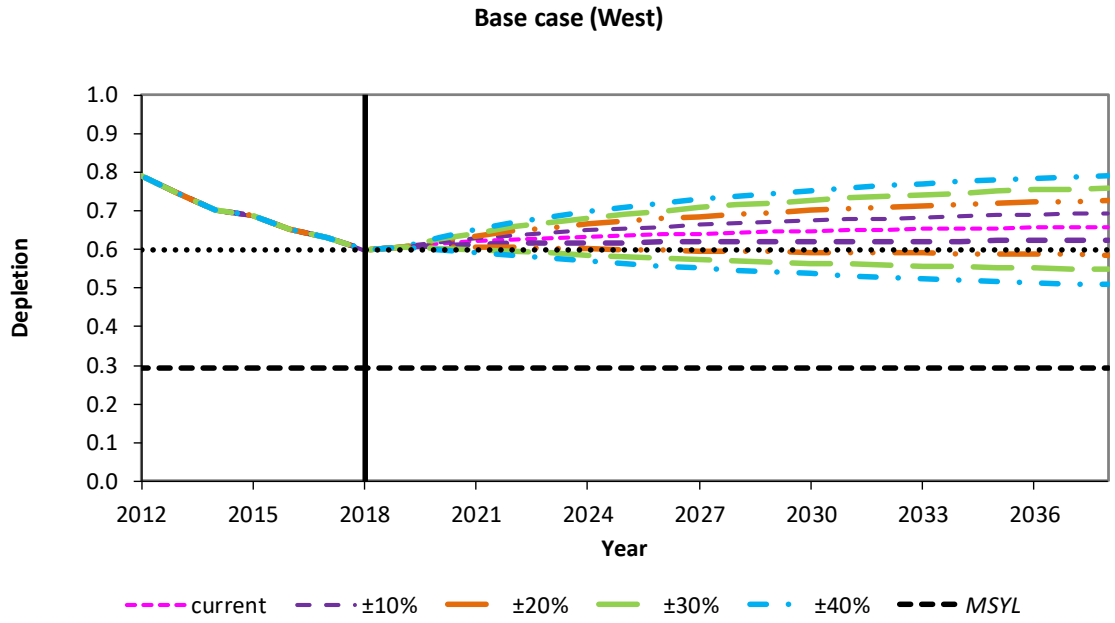

Figure 11a. Spawning biomass depletion projections (shown after the vertical line) under future annual catches of 2 157 tonnes (as for 2018) for the **Base case** for the **West** as well as for several variants of this catch: ±10%, ±20%, ±30% and ±40%. The dotted horizontal line shows the current (2018) depletion value for this assessment model and the dashed horizontal line shows the *MSYL* value.

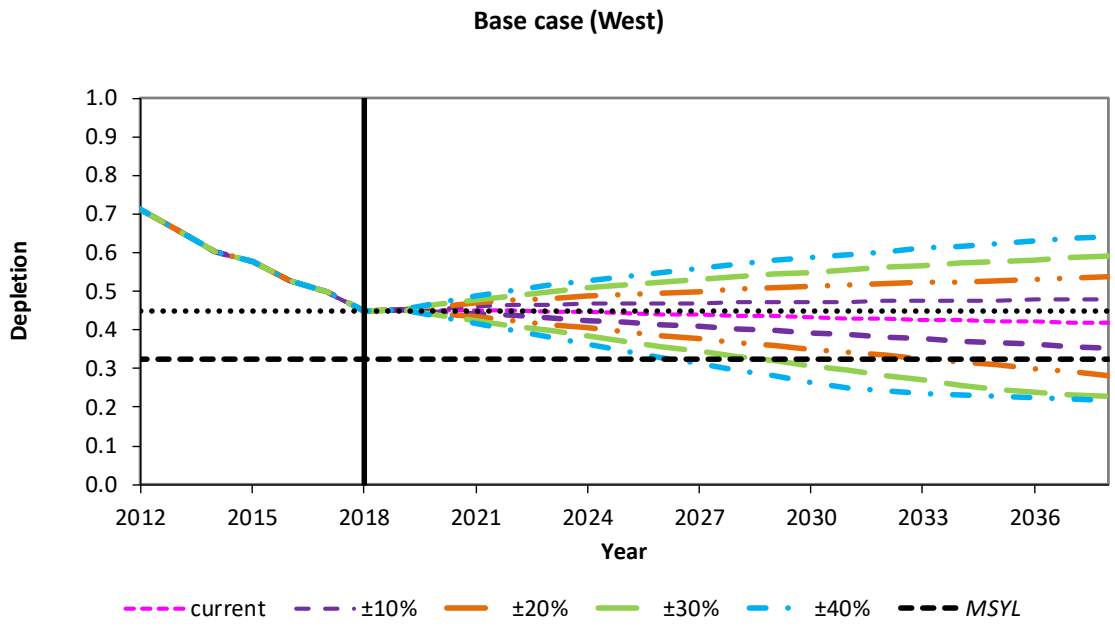

Figure 11b. Spawning biomass depletion projections (shown after the vertical line) under future annual catches of 2 157 tonnes (as for 2018) for the **West** for the **sensitivity** which assumes ***M* = 0.15** as well as projections for several variants of this catch: ±10%, ±20%, ±30% and ±40%. The dotted horizontal line shows the current (2018) depletion value for this assessment model and the dashed horizontal line shows the *MSYL* value.

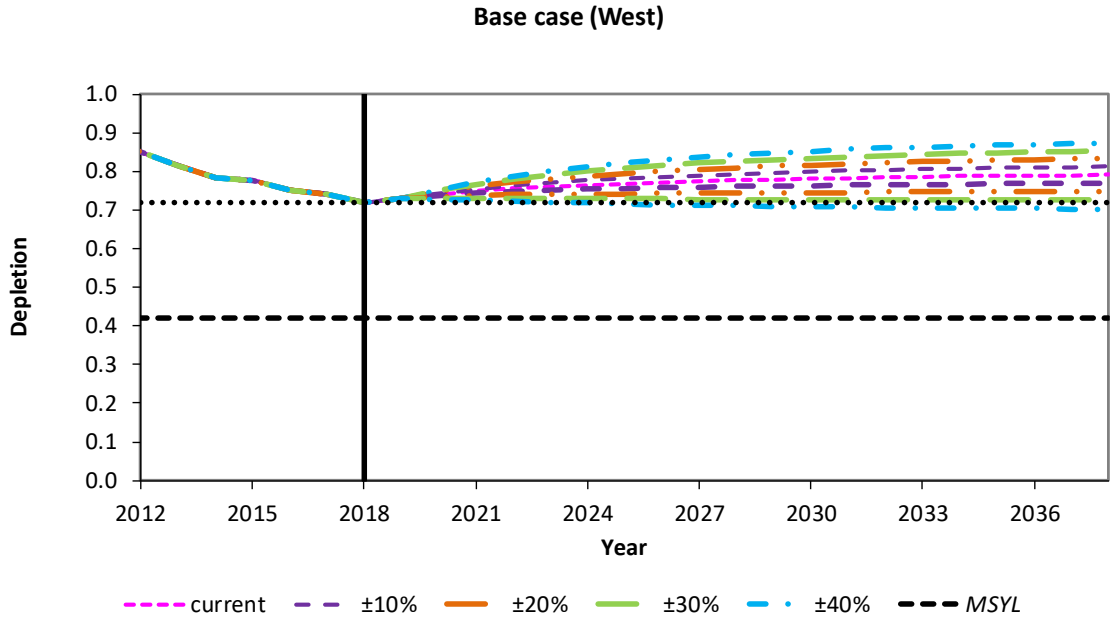

Figure 11c. Spawning biomass depletion projections (shown after the vertical line) under future annual catches of 2 157 tonnes (as for 2018) for the **West** for the **sensitivity** which assumes ***M* = 0.25** as well as projections for several variants of this catch: ±10%, ±20%, ±30% and ±40%. The dotted horizontal line shows the current (2018) depletion value for this assessment model and the dashed horizontal line shows the *MSYL* value.

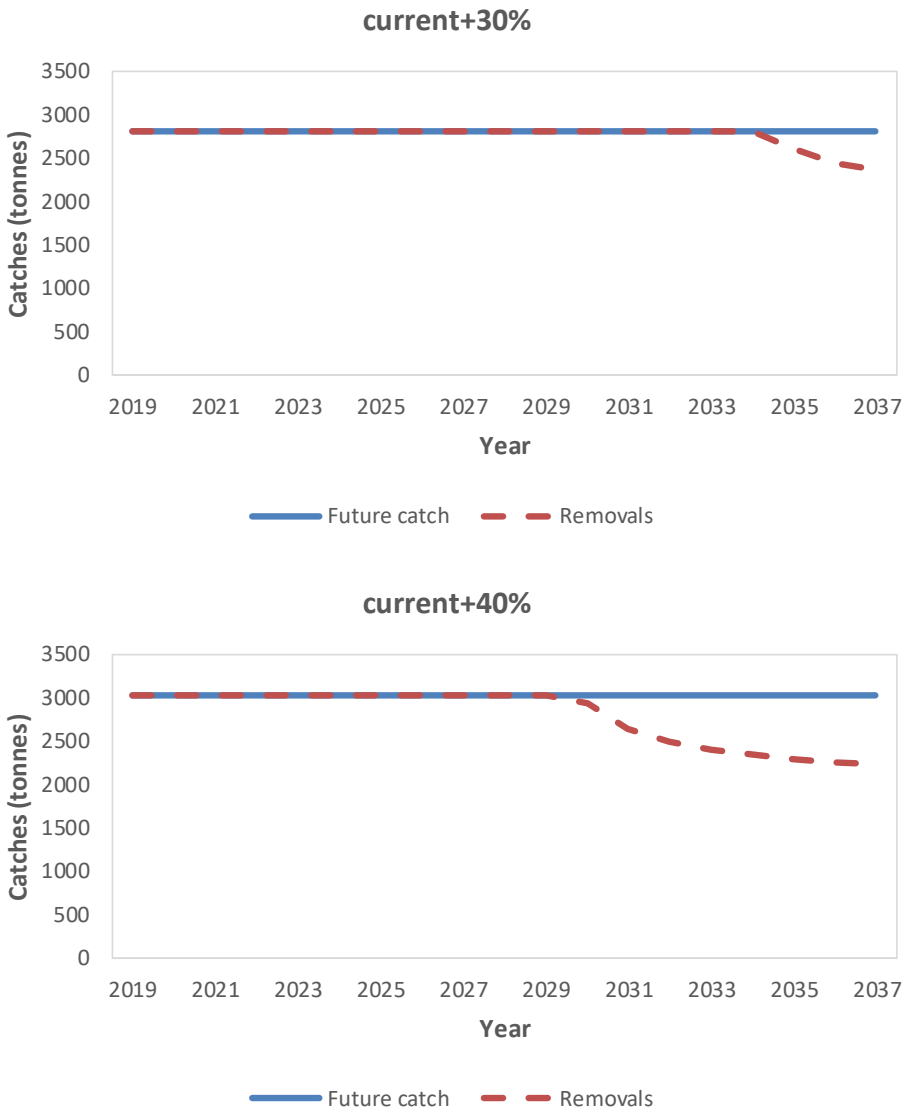

Figure 11d. Base case future **West** area catch levels assumed to remain at +30% (top) and at +40% (bottom) of the 2018 catch level, and the actual removals made for the projections because of the model restriction that does not allow the fully selected fishing proportion to be greater than 90%. Thus, the model builds in a factor to allow for the fact that as abundance declines, it would not be possible to sustain the current catch removals. These results are for the sensitivity when ***M*** **= 0.15**.

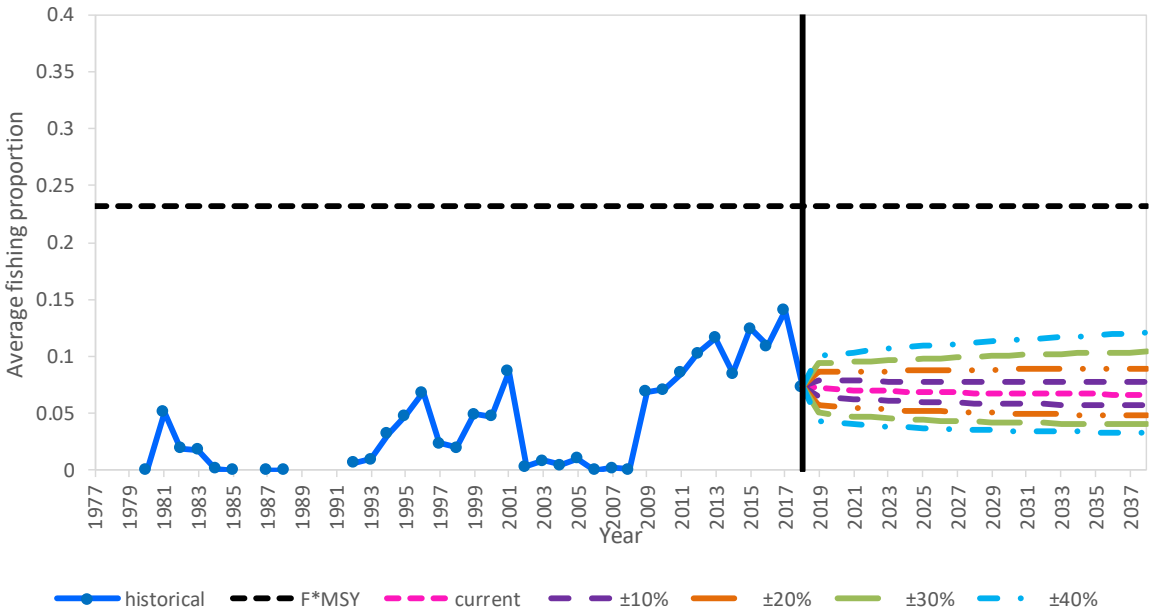

Figure 11e. Average fishing proportion (*F**) trajectories and projections (shown after the vertical line) for the **Base case** for the **West** area. The dashed horizontal line shows F^*_{MSY} for this assessment model.

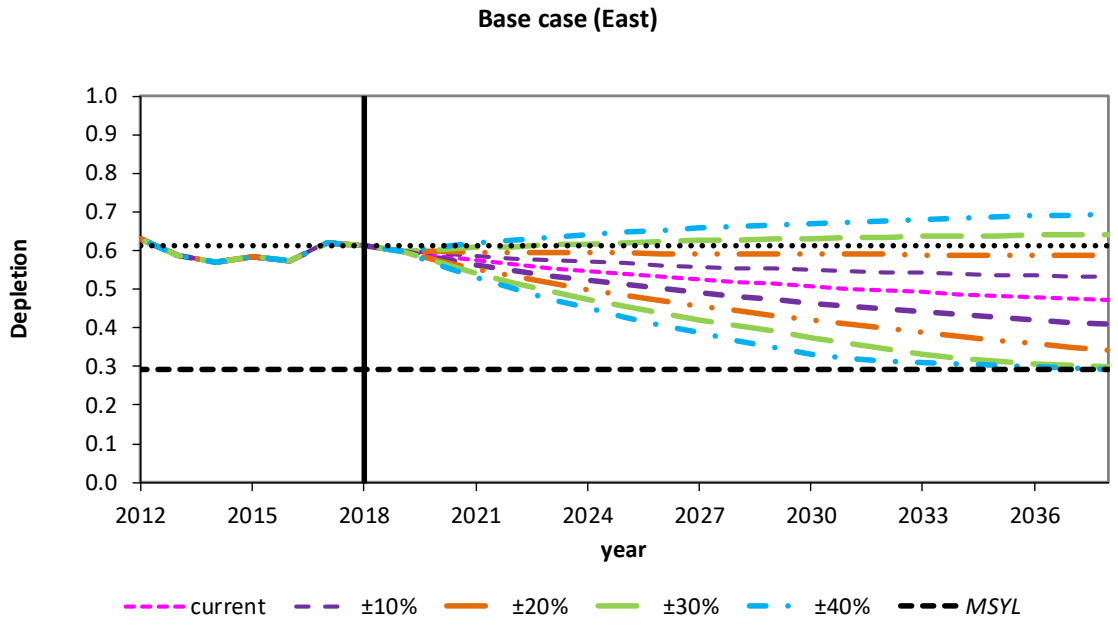

Figure 12a. Spawning biomass depletion projections (shown after the vertical line) under future annual catches of 992 tonnes (as for 2018) for the **Base case** for the **East** as well as for several variants of this catch: ±10%, ±20%, ±30% and ±40%. The dotted horizontal line shows the current (2018) depletion value for this assessment model and the dashed horizontal line shows the *MSYL* value.

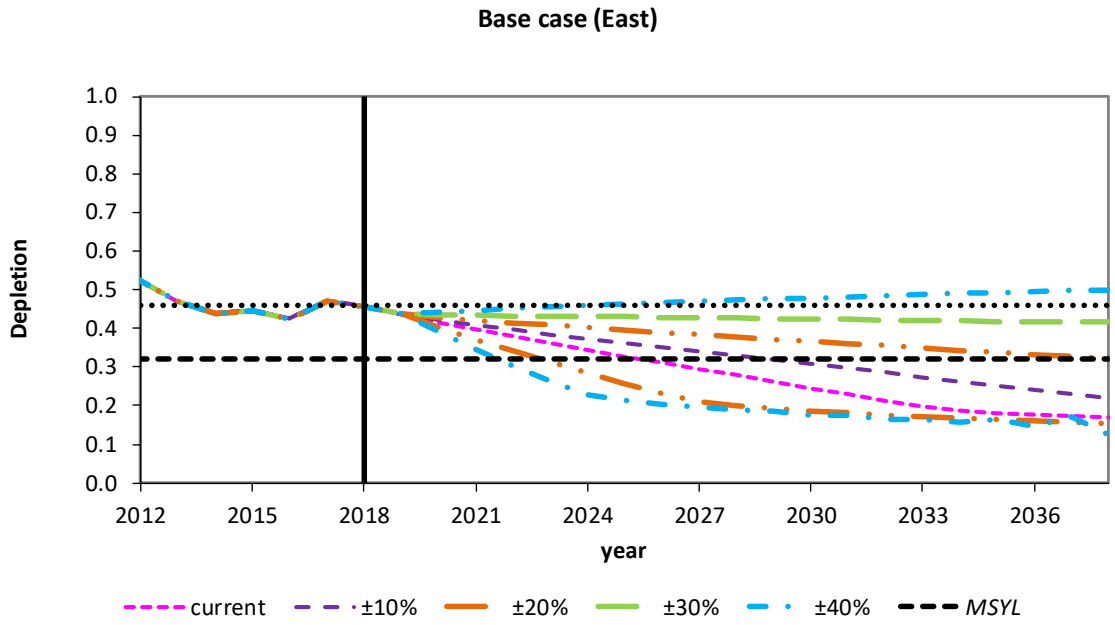

Figure 12b. Spawning biomass depletion projections (shown after the vertical line) under future annual catches of 992 tonnes (as for 2018) for the **East** for the **sensitivity** which assumes ***M* = 0.15** as well as projections for several variants of this catch: ±10%, ±20%, ±30% and ±40%. The dotted horizontal line shows the current (2018) depletion value for this assessment model and the dashed horizontal line shows the *MSYL* value.

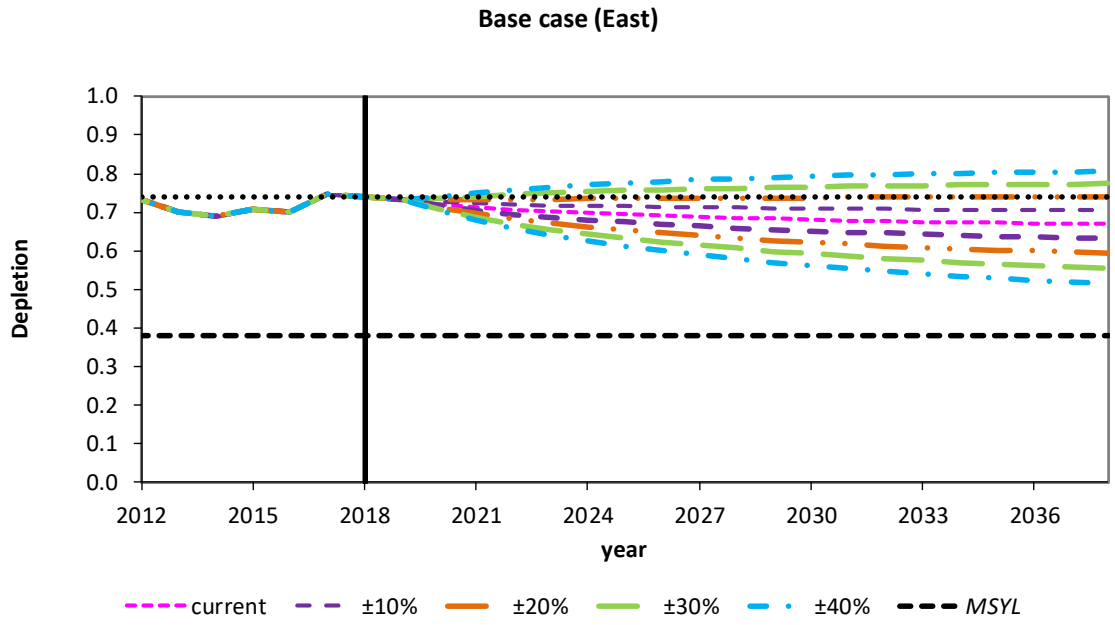

Figure 12c. Spawning biomass depletion projections (shown after the vertical line) under future annual catches of 992 tonnes (as for 2018) for the **East** for the **sensitivity** which assumes ***M* = 0.25** as well as projections for several variants of this catch: ±10%, ±20%, ±30% and ±40%. The dotted horizontal line shows the current (2018) depletion value for this assessment model and the dashed horizontal line shows the *MSYL* value.

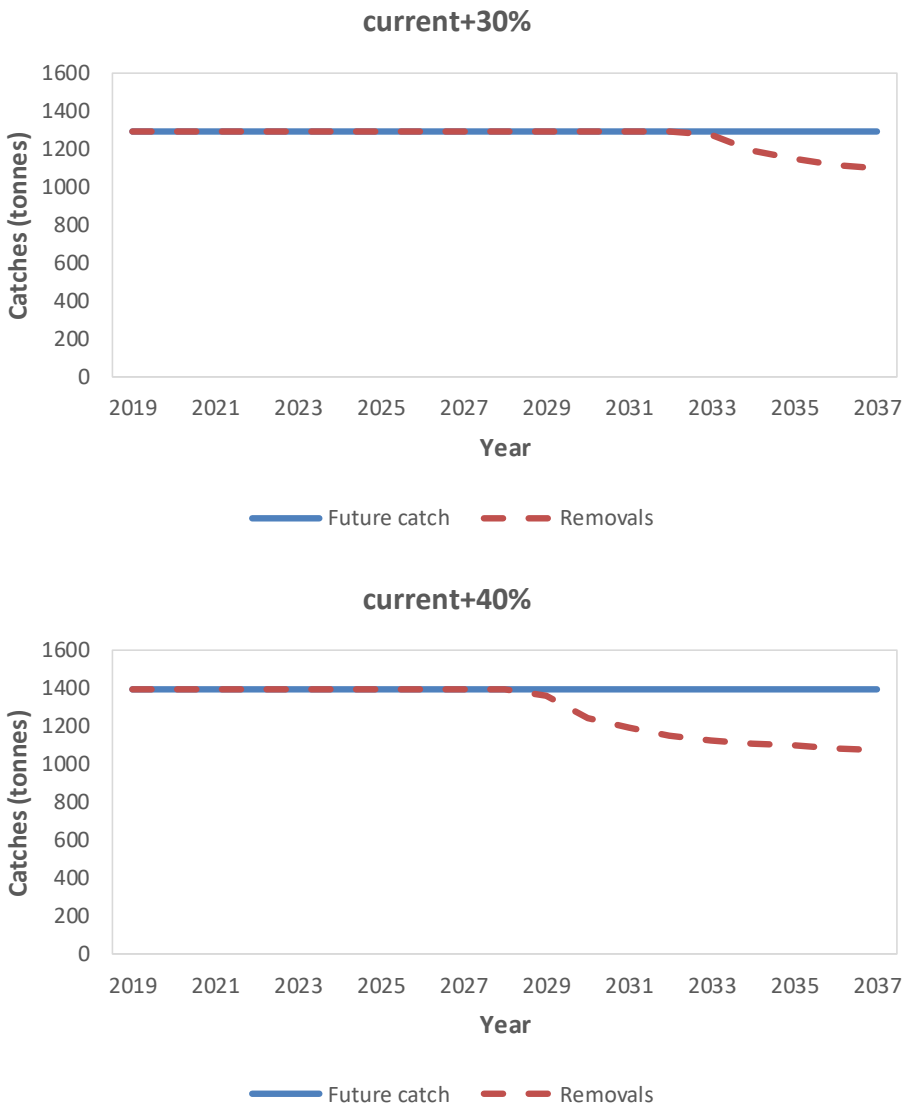

Figure 12d. **Base case** future **East** area catch levels assumed to remain at +30% (top) and at +40% (bottom) of the 2018 catch level, and the actual removals made for the projections because of the model restriction that does not allow the fully selected fishing proportion to be greater than 90%. Thus, the model builds in a factor to allow for the fact that as abundance declines, it would not be possible to sustain current catch removals.

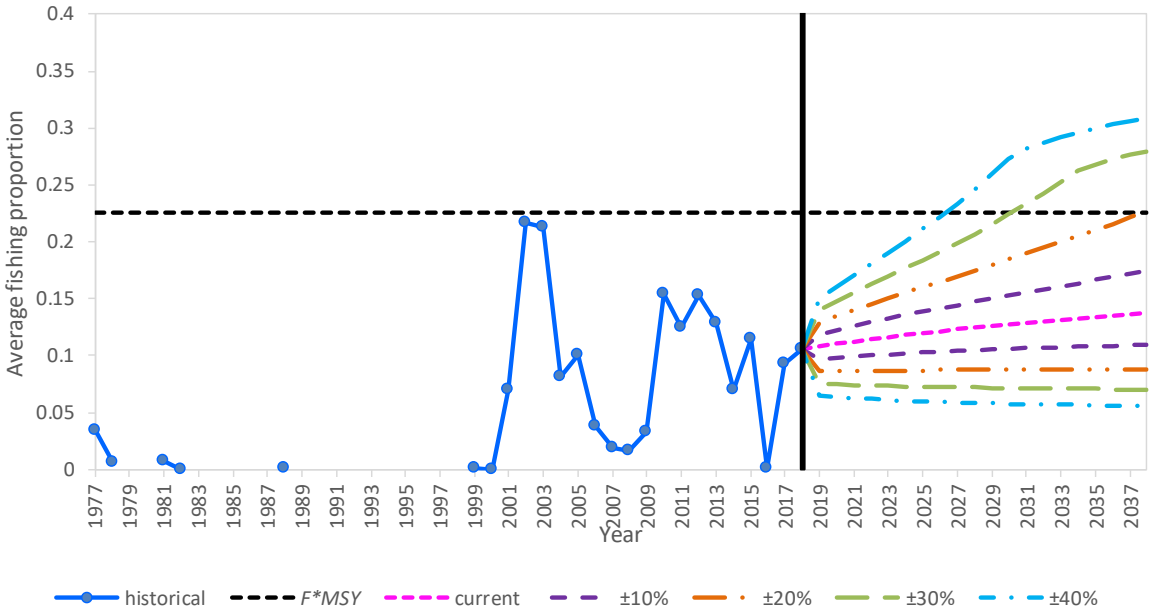

Figure 12e. Average fishing proportion (*F**) trajectories and projections (shown after the vertical line) for the **Base case** for the **East** area. The dashed horizontal line shows F^*_{MSY} for this assessment model.

APPENDIX 1

THE AGE STRUCTURED PRODUCTION MODEL (ASPM) ASSESSMENT METHODOLOGY

THE BASIC DYNAMICS

The Alfonsino population dynamics are described by the equations:

$$N_{y+1,0} = R(B^{sp}_{y+1}) \tag{A1.1}$$

$$N_{y+1,a+1} = (N_{y,a} - C_{y,a})\ e^{-M} \qquad 0 \le a \le m\text{-}2 \tag{A1.2}$$

$$N_{y+1,m} = (N_{y,m} - C_{y,m})\ e^{-M} + (N_{y,m-1} - C_{y,m-1})\ e^{-M} \tag{A1.3}$$

where:

$N_{y,a}$ is the number of Alfonsino of age *a* at the start of year *y*,

$C_{y,a}$ is the number of Alfonsino of age *a* taken by the fleets in year *y*,

$R(B^{sp})$ is the Beverton-Holt stock-recruitment relationship described by equation (A1.10) below,

B^{sp} is the spawning biomass at the start of year *y*,

M is the natural mortality rate of Alfonsino (assumed to be independent of age), and

m is the maximum age considered (i.e. the "plus group"), taken here to be *m* = 25.

Note that in the interests of simplicity, this approximates the fishery as a pulse fishery at the start of the year. Given that Alfonsino are relatively long-lived with low natural mortality, such an approximation would seem adequate.

For a fishery for which CPUE series are available for three different fleets, the total predicted number of fish of age *a* caught in year *y* is given by:

$$C_{y,a} = \sum_{f=1}^{3} C^f_{y,a}, \tag{A1.4}$$

where:

$$C^f_{y,a} = N_{y,a} S^f_{y,a} F^f_y \tag{A1.5}$$

and:

F^f_y is the proportion of the resource above age *a* harvested in year *y* by fleet *f*, and

$S^f_{y,a}$ is the commercial selectivity at age *a* in year *y* for fleet *f*.

The mass-at-age is given by the combination of a von Bertalanffy growth equation $\ell(a)$ defined by constants ℓ_∞, κ and t_0, and a relationship relating length to mass. Note that ℓ refers to fork length.

$$\ell(a) = \ell_\infty[1 - e^{-\kappa(a-t_0)}] \tag{A1.6}$$

$$w_a = c[\ell(a)]^d \tag{A1.7}$$

where:

w_a is the mass of a fish at age *a*.

The fleet-specific total catch by mass in year *y* is given by:

$$C_y^f = \sum_{a=0}^{m} w_a C_{y,a}^f = \sum_{a=0}^{m} w_a \, S_{y,a}^f F_y^f N_{y,a} \tag{A1.8}$$

which can be re-written as:

$$F_y^f = \frac{C_y^f}{\sum_{a=0}^{m} w_a S_{y,a}^f N_{y,a}} \tag{A1.9}$$

FISHING SELECTIVITY

The fleet-specific commercial fishing selectivity, $S_{y,a}^f$, is assumed to be described by a logistic curve. This is given by:

$$S_{y,a}^f = \left[1 + e^{-\left(a - a_{50,y}^f\right)/\delta_y^f}\right]^{-1} \tag{A1.10}$$

where

$a_{50,y}^f$ is the age-at-50% selectivity (in years) for year *y* for fleet *f*, and

δ_y^f defines the steepness of the ascending section of the selectivity curve (in years^{-1}) for year *y* for fleet *f*.

In cases where equation (A1.9) yields a value of $F_y^f > 0.9$ for a future year, i.e. the available biomass is (virtually) less than the proposed catch for that year, F_y^f is restricted to 0.9, and the actual catch considered to be taken will be less than the proposed catch. This procedure would make no adjustment to the exploitation rate $\left(S_{y,a}^f F_y^f\right)$ of other ages. However, to avoid the unnecessary reduction of catches from ages where the TAC could have been taken if the selectivity for those ages had been increased, the following procedure is adopted (CCSBT, 2003).

The fishing mortality, F_y^f, is computed as usual using equation (A1.9). If $F_y^f \leq 0.9$ no change is made to the computation of the total catch, C_y^f, given by equation (A1.8). If $F_y^f > 0.9$, compute the total catch from:

$$C_y^f = \sum_{a=0}^{m} w_a \, g(S_{y,a}^f F_y^f) N_{y,a}. \tag{A1.11}$$

Denote the modified selectivity by $S_{y,a}^{f*}$, where:

$$S_{y,a}^{f*} = \frac{g(S_{y,a}^f F_y^f)}{F_y^f}, \tag{A1.12}$$

so that $C_y^f = \sum_{a=0}^{m} w_a \, S_{y,a}^{f*} F_y^f N_{y,a}$, where

$$g(x) = \begin{cases} x & x \leq 0.9 \\ 0.9 + 0.1\left[1 - e^{(-10(x-0.9))}\right] & 0.9 < x \leq \infty \end{cases}. \tag{A.1.13}$$

Now F_y^f is not bounded above by one, but $g\left(S_{y,a}^f F_y^f\right) \leq 1$ hence $C_{y,a}^f = g(S_{y,a}^f F_y^f) N_{y,a} \leq N_{y,a}$ as required.

STOCK-RECRUITMENT RELATIONSHIP

The spawning biomass in year *y* is given by:

$$B_y^{sp} = \sum_{a=1}^{m} w_a f_a N_{y,a} = \sum_{a=a_m}^{m} w_a N_{y,a} \quad \text{(A1.14)}$$

where:

f_a = the proportion of fish of age *a* that are mature (assumed to be knife-edge at age a_m).

The number of recruits at the start of year *y* is assumed to be related to the spawning biomass at the start of year *y*, B_y^{sp}, by a Beverton-Holt stock-recruitment relationship (note: assuming deterministic recruitment here):

$$R(B_y^{sp}) = \frac{\alpha B_y^{sp}}{\beta + B_y^{sp}}. \quad \text{(A1.15)}$$

The values of the parameters α and β can be calculated given the unexploited equilibrium (pristine) spawning biomass K^{sp} and the steepness of the curve *h*, using equations (A1.16)–(A1.20) below. If the pristine recruitment is $R_0 = R(K^{sp})$, then steepness is the recruitment (as a fraction of R_0) that results when spawning biomass is 20% of its pristine level, i.e.:

$$hR_0 = R(0.2K^{sp}) \quad \text{(A1.16)}$$

from which it can be shown that:

$$h = \frac{0.2(\beta + K^{sp})}{\beta + 0.2K^{sp}}. \quad \text{(A1.17)}$$

Rearranging equation (A1.17) gives:

$$\beta = \frac{0.2K^{sp}(1-h)}{h-0.2} \quad \text{(A1.18)}$$

and solving equation (A1.15) for α gives:

$$\alpha = \frac{0.8hR_0}{h-0.2}.$$

In the absence of exploitation, the population is assumed to be in equilibrium. Therefore R_0 is equal to the loss in numbers due to natural mortality when $B^{sp} = K^{sp}$, and hence:

$$\gamma K^{sp} = R_0 = \frac{\alpha K^{sp}}{\beta + K^{sp}} \quad \text{(A1.19)}$$

where:

$$\gamma = \left\{\sum_{a=1}^{m-1} w_a f_a e^{-Ma} + \frac{w_m f_m e^{-Mm}}{1-e^{-M}}\right\}^{-1}. \quad \text{(A1.20)}$$

PAST STOCK TRAJECTORY AND FUTURE PROJECTIONS

Given a value for the pre-exploitation equilibrium spawning biomass (K^{sp}) of Alfonsino, and the assumption that the initial age structure corresponds to equilibrium, it follows that:

$$K^{sp} = R_0 \left(\sum_{a=1}^{m-1} w_a f_a \, e^{-Ma} + \frac{w_m f_m e^{-Mm}}{1-e^{-M}} \right) \quad \text{(A1.21)}$$

which can be solved for R_0.

The initial numbers at each age *a* for the trajectory calculations, corresponding to the deterministic equilibrium, are given by:

$$N_{0,a} = \begin{cases} R_0 e^{-Ma} & 0 \le a \le m-1 \\ \frac{R_0 e^{-Ma}}{1-e^{-M}} & a = m \end{cases} \quad \text{(A1.22)}$$

Numbers-at-age for subsequent years are then computed using equations (A1.1)-(A1.5) and (A1.8)-(A1.14) under the series of annual catches given (for the past, but also possibly for future projections).

The model estimate of the fleet-specific exploitable component of the biomass is given by:

$$B_y^{\exp}(f) = \sum_{a=0}^{m} w_a S_{y,a}^f N_{y,a} \quad \text{(A1.23)}$$

THE LIKELIHOOD FUNCTION

The age-structured production model (ASPM) is fitted to the fleet-specific GLM standardised CPUE to estimate model parameters. The likelihood is calculated assuming that the observed (standardised) CPUE abundance indices are lognormally distributed about their expected values:

$$I_y^f = \hat{I}_y^f e^{\varepsilon_y^f} \text{ or } \varepsilon_y^f = ln\left(I_y^f\right) - ln\left(\hat{I}_y^f\right), \quad \text{(A1.24)}$$

where:

I_y^f is the standardised CPUE series index for year *y* corresponding to fleet *f*,

$\hat{I}_y^f = \hat{q}^f \hat{B}_y^{\exp}(f)$ is the corresponding model estimate, where:

$\hat{B}_y^{\exp}(f)$ is the model estimate of exploitable biomass of the resource for year *y* corresponding to fleet *f*, and

$\hat{q}^f$ is the catchability coefficient for the standardised commercial CPUE abundance indices for fleet *f*, whose maximum likelihood estimate is given by:

$$\widehat{ln\, q}^f = \frac{1}{n^f} \sum_y \left(ln\, I_y^f - \widehat{ln\, B}_y^{\exp}(f) \right), \quad \text{(A1.25)}$$

where:

n^f is the number of data points in the standardised CPUE abundance series for fleet *f*, and

ε_y^f is normally distributed with mean zero and standard deviation σ^f (assuming homoscedasticity of residuals), whose maximum likelihood estimate is given by:

$$\hat{\sigma}^f = \sqrt{\frac{1}{n^f} \sum_y \left(ln\, I_y^f - \widehat{ln\, q}^f \, \hat{B}_y^{\exp}(f) \right)^2}. \quad \text{(A1.26)}$$

The negative log likelihood function (ignoring constants) which is minimised in the fitting procedure is thus:

$$-ln\, L = \sum_f \left\{ \sum_y \left[\frac{1}{2(\sigma^f)^2} \left(ln\ \ I_y^f \ - \ ln\ \ \left(q^f \ B_y^{\exp}(f) \right) \right)^2 \right] + n^f \left(ln\, \sigma^f \right) \right\}. \quad \text{(A1.27)}$$

The estimable parameters of this model are q^f, K^{sp}, and σ^f, where K^{sp} is the pre-exploitation mature biomass.

EXTENSION TO INCORPORATE CATCH-AT-LENGTH INFORMATION

The model above provides estimates of the catch-at-age ($C^f_{y,a}$) by number made by each fleet in the fishery each year from equation (A1.5). These in turn can be converted into proportions of the catch of age *a*:

$$p^f_{y,a} = \frac{C^f_{y,a}}{\sum_{a'} C^f_{y,a'}}. \tag{A1.28}$$

Using the von Bertalanffy growth equation (A1.6), these proportions-at-age can be converted to proportions-at-length – here under the assumption that the distributions of length-at-age remain constant over time:

$$p^f_{y,\ell} = \sum_a p^f_{y,a} A^f_{a,\ell} \tag{A1.29}$$

where $A^f_{a,\ell}$ is the proportion of fish of age *a* that fall in length group ℓ for fleet *f*. Note that therefore:

$$\sum_\ell A^f_{a,\ell} = 1 \quad \text{for all ages } a. \tag{A1.30}$$

The *A* matrix has been calculated here under the assumption that length-at-age is normally distributed about a mean given by the von Bertalanffy equation, i.e.:

$$\ell(a) \sim N^*\left[\ell_\infty\left\{1 - e^{-\kappa(a-t_0)}\right\};\ \theta^f(a)^2\right] \tag{A1.31}$$

where

N^* is a normal distribution truncated at ± 3 standard deviations (to avoid negative values), and

$\theta^f(a)$ is the standard deviation of length-at-age *a* for fleet *f*, which is modelled here to be proportional to the expected length at age *a*, i.e.:

$$\theta^f(a) \ = \ \beta^f \ell_\infty\left\{1 - e^{-\kappa(a-t_0)}\right\} \tag{A1.32}$$

with β^f a parameter which is estimated in the model fitting process.

Note that since the model of the population's dynamics is based upon a one-year time step, the value of β^f and hence the $\theta^f(a)$'s estimated will reflect not only the real variability of length-at-age, but also the "spread" that arises from the fact that fish in the same annual cohort are not all spawned at exactly the same time, and that catching takes place throughout the year so that there are differences in the age (in terms of fractions of a year) of fish allocated to the same cohort.

Model fitting is then achieved by adding the following term to the negative log-likelihood of equation (A1.27):

$$-\ln L_{len} = w_{len} \sum_{f,y,\ell} \left\{ ln\left[\frac{\sigma^f_{len}}{\sqrt{p^f_{y,\ell}}}\right] + \left(\frac{p^f_{y,\ell}}{\left(2\left(\sigma^f_{len}\right)^2\right)}\right)\left[ln\, p^{obs}_{y,\ell}(f) - ln\, p^f_{y,\ell}\right]^2 \right\} \tag{A1.33}$$

where

$p^{obs}_{y,\ell}(f)$ is the proportion by number of the catch in year *y* in length group ℓ for fleet *f*, and

σ_{len}^{f} has a closed form maximum likelihood estimate given by:

$$\left(\hat{\sigma}_{len}^{f}\right)^2 = \frac{\sum_{y,\ell} p_{y,\ell}^{f}\left[ln\, p_{y,\ell}^{obs}(f) - ln\, p_{y,\ell}^{f}\right]^2}{\sum_{y,\ell} 1}. \quad \text{(A1.34)}$$

Equation (A1.33) makes the assumption that proportions-at-length data are log-normally distributed about their model-predicted values. The associated variance is taken to be inversely proportional to $p_{y,\ell}^{f}$ to downweight contributions from expected small proportions which will correspond to small observed sample sizes. This adjustment (known as the Punt-Kennedy approach) is of the form to be expected if a Poisson-like sampling variability component makes a major contribution to the overall variance.

The w_{len} weighting factor may be set at a value less than 1 to down-weight the contribution of the catch-at-length data to the overall negative log-likelihood, compared to that of the CPUE data in equation (A1.27). The reason that this factor is introduced is that the $p_{y,\ell}^{obs}(f)$ data for a given year frequently show evidence of strong positive correlation, and so would not be as informative as the independence assumption underlying the form of equation (A1.33) would otherwise suggest.

In the practical application of equation (A1.33), length observations were grouped by 1 cm intervals, with minus- and plus-groups specified below 20 and above 50 cm respectively.